The Pennsylvania State University

The Graduate School

Eberly College of Science

INVESTIGATIONS IN QUANTUM MONTE CARLO

A Thesis in

Chemistry

by

Matthew Clifford Wilson

Submitted in Partial Fulfillment
of the Requirements
for the Degree of

Doctor of Philosophy

May 2007

The thesis of Matthew Clifford Wilson was reviewed and approved* by the following:

James B. Anderson
Professor of Chemistry
Thesis Advisor
Chair of Committee

Mark Maroncelli
Professor of Chemistry

John V. Badding
Professor of Chemistry

Jainendra K. Jain
Professor of Physics

Ayusman Sen
Professor of Chemistry
Head of the Department of Chemistry

*Signatures are on file in the Graduate School.

ABSTRACT

A scheme to calculate a correction to the energy obtained by the variational quantum Monte Carlo (VQMC) method by using the diffusion quantum Monte Carlo (DQMC) method is applied to three systems, neon, H_2, and cyclical C_{10}. This scheme has the advantage that the time step error incurred in the use of the DQMC method is minimized since it only applies to the correction to the energy, rather than the entire energy.

The simulation for neon validated the use of the scheme in correctly calculating the ground state energy of an atom. In this case, the scheme obtained 97% of the difference in energy between the VQMC and DQMC energies. The simulation for H_2 was done to reproduce results of a simple, well-known system for various bond lengths. Again, in this case, the correction scheme succeeded in correcting the VQMC energy to close to the DQMC values. Finally, for cyclical C_{10}, the scheme was run for a number of geometries in which either the bond angles or bond lengths were varied at different ring sizes. It was found that for smaller rings, a more symmetrical geometry is preferred, while for larger ring sizes there tend to be at least a local minimum energy for rings distorted by either their bond angles or bond lengths.

Also included are DQMC calculations of the potential energies of interaction of helium atoms in helium dimers and trimers. Statistical errors are lower by a factor of two to ten than for earlier diffusion calculations. The calculations for the trimers reveal interaction energies very nearly pairwise-additive for internuclear distances near the dimer equilibrium distance of 5.6 bohr and longer.

TABLE OF CONTENTS

LIST OF TABLES

LIST OF FIGURES

ACKNOWLEDGEMENTS

CHAPTER 1

QUANTUM MONTE CARLO

Monte Carlo Methods

In 1931, five years after he developed wave mechanics, in 1931, Schrödinger reported the relation between the Schrödinger equation in imaginary time and the equation that governs particles undergoing diffusion.[1] The first application of the Monte Carlo method to this relation was by Metropolis and Ulam in 1949, creating the diffusion quantum Monte Carlo method.[2] In 1962, Kalos observed that the Schrödinger equation could be transformed from a differential equation into an integral equation for which the Green's function is known in the case of the wavefunction vanishing at infinity.[3] This was the introduction of Green's function quantum Monte Carlo. Although already applied to other systems, the variational quantum Monte Carlo method was first used to study molecular systems in 1964, by Conroy.[4] In four papers, he reported results for H_2^+, HeH^{2+}, HeH^+, H_3^{2+}, and H_3^+.

Monte Carlo methods are a set of techniques that simulate behavior of a system stochastically, usually through the use of random number sequences. In looking at physical systems, they are often applied to ones with a large number of strongly coupled degrees of freedom, such as fluids and disordered materials. These methods are also useful in studying mathematical systems, particularly for evaluating high dimensional integrals and classes of equations difficult to solve

by standard analytical and numerical methods, one such equation being the Schrödinger equation.

One important Monte Carlo technique is the random walk. In this method, collections of points in space called "walkers" are moved around randomly according to a desired probability distribution. A common way to direct the walks so that they conform to this probability distribution is the Metropolis algorithm.[5] In the algorithm, each move in the walk is proposed at random, using a uniform probability distribution. Then, the move is accepted with probability min(1, $\rho(X_{new})/\rho(X_{old})$), where $\rho(X_{old})$ is the probability for the system to be in state X_{old} and $\rho(X_{new})$, the probability for the system to be in state X_{new}. This means the walker always accepts the move if it is to a state with a higher probability, and accepts the move if it is to a state with lower probability with a probability equal to the ratio of the new probability to the old probability.

In Monte Carlo integration, the value of a definite integral is approximated by the average value of the integrand at various points within the upper and lower limits multiplied by the range of the limits. These points are randomly drawn from a probability density function, often times involving the Metropolis algorithm. This technique has an advantage over grid or weighting methods at high dimensions because of how rapidly the computational effort rises for these latter methods.

Variational Quantum Monte Carlo

The variational principle states that the expectation value of the energy, E_1 of a trial wave function ψ_0 is a minimum when ψ_0 is the exact ground state wave function, where:

$$E_1 = \frac{\int \psi_0^* H \psi_0 \, d\mathbf{x}}{\int \psi_0^* \psi_0 \, d\mathbf{x}} \tag{1.1}$$

This equation gives a strict upper bound to the exact ground state energy. In variational quantum Monte Carlo (VQMC), E_1 is evaluated using Monte Carlo integration. In this method, Equation (1) is rewritten as:

$$E_1 = \frac{\int \psi_0^2 E_{loc} \, d\mathbf{x}}{\int \psi_0^2 \, d\mathbf{x}} \tag{1.2}$$

where E_{loc} is defined as:

$$E_{loc} = \frac{H\psi_0}{\psi_0} \tag{1.3}$$

and is termed the "local energy". Rewriting E_1 in this way puts it into the form of a weighted average, with the weight being the normalized probability density function of the electrons. The sample points are then taken from the distribution ψ_0^2 by Metropolis sampling and the Monte Carlo estimate of the energy is just the average of the local energies for each sample point.

Diffusion Quantum Monte Carlo

The time-dependent Schrödinger equation for one particle in one dimension is:

$$-i\hbar \frac{\partial \psi}{\partial t} = \frac{\hbar^2}{2\mu} \frac{\partial^2 \psi}{\partial x^2} - V\psi \tag{1.4}$$

where ψ is the wave function of the particle, $\hbar$ is Planck's constant, μ is the particle's mass, and V is the potential energy of the particle. This equation can be converted into an ordinary differential equation with real variables by a transformation to imaginary time τ which is defined as $it/\hbar$:

$$\frac{\partial \psi}{\partial \tau} = \frac{\hbar^2}{2\mu} \frac{\partial^2 \psi}{\partial x^2} - V\psi \tag{1.5}$$

Equation (1.5) has a similar form to the diffusion equation:

$$\frac{\partial C}{\partial t} = D \frac{\partial^2 C}{\partial x^2} \tag{1.6}$$

where C is the concentration of the diffusing species and D is the diffusion coefficient. The diffusion of particles can be simulated by a random walk process in which the diffusing particles are moved in a time interval Δt a distance Δx in a random direction. The step sizes Δt and Δx are related to the diffusion coefficient by the Einstein equation[6]:

$$D = \frac{1}{2} \frac{(\Delta x)^2}{\Delta t} \tag{1.7}$$

In effect, this simulation solves the differential equation in (1.6). With the addition of a first-order rate term to Equation (1.6), such as in the case of

4

diffusion combined with chemical reaction, the diffusion equation has a form

identical to (1.5):

$$\frac{\partial C}{\partial t} = D\frac{\partial^2 C}{\partial x^2} - kC \qquad (1.8)$$

where k is the rate constant of the chemical reaction. This process can be

simulated in the same way as for (1.6) with the additional step of subjecting the

particles to disappearance or multiplication with a probability proportional to k or

$- k$, respectively. Equations (1.5) and (1.8) have the same form: $\psi \leftrightarrow C$, $\tau \leftrightarrow t$,

$\hbar^2/2\mu \leftrightarrow D$, and $V \leftrightarrow k$. Because of this, the same process for simulating diffusion

with chemical reaction can be used to solve the differential equation in (1.5).[7]

This process is called diffusion quantum Monte Carlo (DQMC).

The DQMC process for solving the Schrödinger equation in one

dimension proceeds as follows: An initial collection of particles (called

ψ-particles) is distributed along the x-axis. Next, each ψ-particle is moved one

step Δx. The direction in which the ψ-particle moves is chosen at random, with

the probability of moving in the positive direction and the probability of moving

in the negative direction both equal to ½. Each ψ-particle then either gives birth

to a new ψ-particle with probability $P_b = - V\Delta\tau$ if V is negative or disappears with

probability $P_b = V\Delta\tau$ if V is positive. The time is advanced one step Δt and the

process is repeated. In this case, Equation (1.7) gives the relationship between Δt

and Δx as:

$$\Delta t = \frac{\mu}{\hbar^2}(\Delta x)^2 \qquad (1.9)$$

As the simulation progresses, the normalized distribution of ψ-particles approaches a "steady-state" distribution which fluctuates about an average steady-state distribution. This distribution corresponds to the lowest energy wave function satisfying the time-independent Schrödinger equation. By generalizing this method to multiple dimensions, the Schrödinger equation can be solved for molecules with any number of electrons.

Comparison to Other Methods

A third type of quantum Monte Carlo method, not applied in this research, is "exact" quantum Monte Carlo (EQMC).[8] In this method, a collection of positive and negative walkers are used to produce a distribution that represents the wave function. In the process, positive and negative walkers in close proximity to each other are cancelled based on probabilities. An advantage of EQMC is that it does not use the fixed-node approximation, but a disadvantage is that the computational requirements limit the application of the method to systems having a very small number of electrons. In general, QMC methods scale as the third power of the number of electrons in the system.

QMC methods are one way of handling the effects of electron correlation, most of the time using wave functions which explicitly incorporate electron-electron terms. The issue of electron correlation stems from the simple theoretical model for electronic structure, in which each electron moves in the average field of all the other electrons. This model forms the basis of Hartree-Fock self-consistent field (SCF) theory. Calculations using this theory account for the

6

majority of the total energy of a molecule, but fail to account for the instantaneous interactions between electrons, called electron correlation. The computational dependence for this method scales as the second to third power of the number of electrons in the system.

Another way to handle electron correlation is to treat it as a perturbation on the SCF theory. This is done in Møller-Plesset (MP) theory by expanding the wave function and energy in a power series of the perturbation. The series is truncated at term of particular order, indicated by the number attached to the end of the method abbreviation, such as MP2 (second-order) and MP4 (fourth-order). The computational dependence for this method increases strongly with the order of perturbation; MP2, MP3, MP4, and MP5, scale as the fifth, sixth, seventh, and eighth power of the number of electrons in the system, respectively.

Another method developed to deal with electron correlation is configuration interaction (CI). In this method, the wave function is taken to be a linear combination of possible electronic configurations. If all possible configurations are included, the method is called full configuration interaction (FCI). This would give the exact solution within a basis set, but since the number of possible electronic configurations increases exponentially with the number of electrons, it is only able to be used for small molecules. For larger molecules, the number of included configurations must be truncated. Usually, this is done by only including single and double excitations, referred to as CISD. The computational dependence for this method scales as the sixth power of the number of electrons in the system. One problem with CISD is that it is not size-

consistent, meaning the calculated energy of a system of noninteracting fragments is not equal to the sum of the calculated energies of the individual fragments.

One method developed to fix this size-consistency problem, is the coupled cluster (CC) method. In relation to CISD, CCSD uses a form of the wave function in which the single and double excitation operators are written as exponentials, allowing the method to be size-consistent. Like CISD, the computational dependence for CCSD scales as the sixth power of the number of electrons in the system.

Finally, density functional theory (DFT) is another way to treat electron correlation. In this method, the electron correlation is taken to be a functional of the three dimensional electron density. The exact functional is not known, so various approximate functionals have been developed. One advantage of DFT is that the computational dependence for certain algorithms scales as the second to third power of the number of electrons in the system. The disadvantage is that the calculations are not as accurate as other methods due to not knowing the exact functional. The major use of this method is for very large systems, where the other electron correlation methods are too computationally demanding.

CHAPTER 2

CORRECTIONS TO DQMC

Difference Functions and Importance Sampling

The DQMC method is simple, but it requires the simulation to run for a very long time in order to accurately determine the energy of a system. A modification to the method, using difference functions as formulated by Anderson and Freihaut[9], allows the direct calculation of the difference between the true wave function ψ and a trial wave function ψ_0, $\delta = \psi - \psi_0$. Substituting δ into (1.5) gives:

$$\frac{\partial \delta}{\partial \tau} = \frac{\hbar^2}{2\mu}\nabla^2\delta - (V - V_{ref})\delta + \frac{\hbar^2}{2\mu}\nabla^2\psi_0 - (V - V_{ref})\psi_0 \qquad (2.1)$$

Another modification to DQMC is to use importance sampling.[10] By using a function defined as the product of the true wave function and a trial wave function, $f = \psi\psi_0$, Equation (1.5) can be transformed into:

$$\frac{\partial f}{\partial \tau} = \frac{1}{2}\nabla^2 f - \nabla\cdot\left(f\nabla\ln\psi_0\right) - \left(E_{loc} - E_{ref}\right)f \qquad (2.2)$$

where ψ_0 is an approximation to the wave function and E_{ref} is a reference energy. This use of a trial function allows the wave function to be sampled more accurately; more samples are taken from the more important parts of the wave function.

Correction Scheme

Another function can be defined as $g = \delta\psi_0 = (\psi - \psi_0)\psi_0$, which is the importance sampling method used on the difference function $\delta = (\psi - \psi_0)$. This transforms the time-independent Schrödinger equation into:

$$\frac{\partial g}{\partial \tau} = \frac{1}{2}\nabla^2 g - \nabla\cdot(g\nabla\ln\psi_0) - (E_{\text{loc}} - E_{\text{ref}})g + \left[-\left(E_{\text{loc}} - E_{\text{ref}}\right)\psi_0^2\right] \qquad (2.3)$$

The final term acts as a distributive source and may be positive or negative. This term, S, can be written as a collection of terms containing the expectation value of the energy of the trial function, E_{var}:

$$S = \left[-\left(E_{\text{loc}} - E_{\text{var}}\right)\psi_0^2\right]_p + \left[-\left(E_{\text{loc}} - E_{\text{var}}\right)\psi_0^2\right]_n + \left[-\left(E_{\text{var}} - E_{\text{ref}}\right)\psi_0^2\right] \qquad (2.4)$$

where p indicates a region where $E_{\text{loc}} < E_{\text{var}}$, which is a positive particle feed, and n indicates a region where $E_{\text{loc}} > E_{\text{var}}$, which is a negative particle feed. The third term is an additional particle feed, usually negative.

Previously,[11] Equation (2.3) was simulated by g-particles continuously fed into the system as dictated by the source terms. These particles were allowed to diffuse, drift, and multiply or disappear. Then, if older than a specified age, positive and negative ones were allowed to cancel each other out regardless of position. The correction term g was then determined by sampling the particle distribution once the system reached a steady state and the energy was given as equal to the reference energy needed to maintain a fixed net weight of particles.

For the current procedure, the integrals of each of the terms in the equation are considered over all space. These integrals are defined as:

$$I_g = \int g \, dV$$

$$I_p = \int \left[-\left(E_{\text{loc}} - E_{\text{var}} \right) \psi_0^2 \right]_p dV$$

$$I_n = \int \left[-\left(E_{\text{loc}} - E_{\text{var}} \right) \psi_0^2 \right]_n dV \qquad (2.5)$$

$$I_q = \int \psi_0^2 \, dV$$

Equation (2.3) then becomes:

$$\frac{\partial I_g}{\partial \tau} = \int \frac{1}{2} \nabla^2 g \, dV - \int \nabla \cdot (g \nabla \ln \psi_0) \, dV$$

$$- \int (E_{\text{loc}} - E_{\text{ref}}) g \, dV + I_g + I_n - (E_{\text{var}} - E_{\text{ref}}) I_q \qquad (2.6)$$

The first term is a diffusion term and the second term is a drift term. These terms only move particles around inside the volume and the drift term keeps the particles from crossing any nodal surface. This means their integral terms do not contribute to changes in I_g and are zero. The third term is a multiplication term; it applies to each particle fed into the system. For each type of particle, an average growth factor over the course of its lifetime in the system can be combined with the feed terms. This gives:

$$\frac{\partial I_g}{\partial \tau} = I_g \overline{f}_p + I_n \overline{f}_n - (E_{\text{var}} - E_{\text{ref}}) I_q \overline{f}_q \qquad (2.7)$$

Since particles fed into the system tend to the same distribution the longer they have been in the system, regardless of the point at which they were fed, those that are old enough may be cancelled in equal weights, positive with negative, no matter their positions. At steady state, $\partial I_g / \partial \tau = 0$, which gives:

$$E = E_{\text{ref}} = E_{\text{var}} - \frac{I_p \bar{f}_p + I_n \bar{f}_n}{I_q \bar{f}_q} \tag{2.8}$$

This equation can be rewritten as:

$$E = E_{\text{ref}} = E_{\text{var}} - \frac{\dfrac{I_p}{I_q} \bar{f}_p + \dfrac{I_n}{I_q} \bar{f}_n}{\bar{f}_q} \tag{2.9}$$

The energy can then be calculated from the ratios of the integrals and the average growth factors as well as E_{var}. The ratios of the integrals can be calculated by using the Metropolis algorithm with ψ_0^2, accumulating the average values of the ratios. From the same calculation, E_{var}, may be determined. The values of the average growth factors are calculated for sample feed particles obtained from the Monte Carlo integrations of ψ_0^2. A particle is selected with a probability proportional to both ψ_0^2 and the absolute value of either $[-(E_{\text{loc}} - E_{\text{var}})]_p$ for p, $[-(E_{\text{loc}} - E_{\text{var}})]_n$ for n, or unity for q. These particles are then subjected to diffusion, drift, and multiplication for a time long enough so that their average weights are constant. Positive particles are fed into regions where $E_{\text{loc}} < E_{\text{var}}$ and give average growth factors greater than unity. Negative particles are fed into regions where $E_{\text{loc}} > E_{\text{var}}$ and give average growth factors less than unity. Particles of type q typically give an average growth factor very close to unity.

This procedure has the advantage of reducing the error from a traditional fixed-node diffusion calculation. The benefit arises because, if the variational energy is known to a high degree of accuracy, the error from the calculation, mainly time-step error, is only in the correction to the trial wave function, rather than the wave function itself. When the trial wave function is a good

approximation to the true wave function, the correction term is small and any error in the correction term is correspondingly small. As the trial wave function approaches the true wave function, the integral ratios approach zero and the average growth factors approach unity.

Fixed-node Approximation

The major problem with DQMC methods is that the density of the walkers, which is always a positive value, represents the wave function, which can have positive and negative regions. This is due to the fundamental requirement that the electronic wave function be antisymmetric with respect to the exchange of any two electrons. In order to simulate an electronic system, a positive walker density must be maintained, while at the same time, this antisymmetry condition must be enforced.

In order to enforce the antisymmetry, a method called the fixed-node approximation is used. To see why, look at equation 2.2. From this equation, f is a density, therefore it must always be positive. This condition implies the boundary condition $f = \psi\psi_0 \geq 0$, which further implies that ψ and ψ_0 change sign together, giving them the same nodes. During the simulation, this boundary condition can be imposed by fixing the nodes of ψ to be the same as those of ψ_0. This is done by rejecting any proposed move of a walker in which it ends up on the other side of a node of ψ_0. The solution given by this method is then an approximation to the exact ground state; if the nodes of ψ_0 were the nodes of ψ, the result would be the exact ground state.

The fixed-node approximation is fairly insensitive to the quality of ψ_0.[12] To see this, a perturbation theory argument relating the fixed-node energy to node defects can be used. Let ψ be given as:

$$\psi = \psi_0 + \lambda\psi_1 + \lambda^2\psi_2 + \lambda^3\psi_3 + \cdots \tag{2.10}$$

where λ is the nodal "perturbation" and ψ_1, ψ_2, ψ_3, $\cdots$ are the first-order, second-order, third-order, … wave functions orthogonal to ψ_0. The zeroth-order energy is the fixed-node energy. The first-order energy is zero, seen by:

$$E^{(1)} = \left\langle \lambda\psi_1 \left| H \right| \psi_0 \right\rangle + \left\langle \psi_0 \left| H \right| \lambda\psi_1 \right\rangle = 2\lambda E^{(0)} \left\langle \psi_1 \middle| \psi_0 \right\rangle = 0 \tag{2.11}$$

where the last equality is due to the orthogonality of ψ_0 and ψ_1. Therefore, the first nonzero energy correction is second-order in the nodal defect.

One property of the energy resulting from a simulation using the fixed-node approximation is that it is a variational upper bound to the true ground state energy.[11] To see this, divide the $3N$-dimensional space for a system of N electrons into its nodal volumes, designated as v_i. Within each v_i, there is a ground-state solution, ψ_i, with energy ε_i satisfying the Schrödinger equation inside the volume and being zero outside the volume. Each ε_i is an upper bond to the ground state energy, as can be shown by constructing a global antisymmetric wave function by permutations of the solution from v_i:

$$\Psi^{(i)}(\mathbf{x}) = \sum_P (-1)^P \psi_i(\Pi\mathbf{x}) \tag{2.12}$$

where Π is the permutation operator on the electrons, P is its eigenvalue, and $(-1)^P$ is +1 for even permutations and −1 for odd permutations. Each $\Psi^{(i)}$ covers

all space with replicas of ψ_i, giving an expectation value of ε_i. The variational principle implies that this must be a variational upper bound to the true ground state energy. If all v_i are equivalent, then $\Psi^{(1)} = \Psi^{(2)} = \Psi^{(3)} = \cdots = \Psi^{(n)}$, and the fixed-node energy would be equal to ε_i. If all v_i are not equivalent, then the walker populations in the higher energy volumes will decrease relative to that of the minimum energy volume, until only the minimum energy volume is populated, giving the fixed-node energy as ε_{min}. In either case, the fixed-node energy is an upper bound to the exact ground state energy.

The process of rejecting a move that ends on the other side of a node does introduce some error into the calculations because of node crossing and recrossing. This happens when a walker's move appears to keep it in the same nodal region, but the path it would have taken if using smaller time steps would have had it crossing a node and then crossing back. This can be corrected for by decreasing a walker's step size as it approaches a node.

CHAPTER 3

HELIUM DIMERS AND TRIMERS

Introduction

In order to carry out simulations of helium clusters and bulk liquid helium, a good model of the weak interaction potential is necessary. When developing this model, it is important to determine whether it is valid to consider the interactions between helium atoms as pairwise additive. If it is not valid, then one must find out in what way and how much the nonpairwise interactions contribute to the interaction potential. These nonpairwise interactions come from dispersion forces and contribute higher order terms to the interaction potential. For the helium trimer with internuclear distances close to the equilibrium distance of the helium dimer, 5.6 bohr, the interaction is expected to be very close to the sum of the interactions between the three pairs of atoms. The higher order terms are thought to be very small and comprise the nonadditive contribution to the total energy of the cluster.

Attractive forces between helium atoms are due to fluctuating electric moments, which induce dipoles in nearby atoms (London dispersion forces). A potential curve for the interaction between two helium atoms was first estimated in a very approximate calculation by Slater[13] in 1928 and gave a minimum of -8.9 K at a distance of 5.6 bohr. Since then, various methods have been used to calculate the energies of different helium clusters with interesting and varied results. For example, early SCF calculations of the dimer with small basis sets

predicted no attraction. When it became possible to use larger basis sets, an attractive well was predicted in agreement with experiment. But even larger basis sets failed to produce an attractive interaction. This odd behavior was largely the result of basis set superposition error, a difficulty encountered in many types of calculations of weak interactions. Modern high-level calculations by a variety of methods, including 'exact' QMC, have given highly accurate and consistent predictions of the potential energy curve for the dimer.[14]

The first perturbative calculations for the trimer were made by Axilrod and Teller[15] and Muto[16] in 1943. Their third-order perturbation expansion is known as the Axilrod-Teller-Muto (ATM) expression. In 1953, Rosen[17] used the valence bond method to calculate the repulsive part of the interaction. Shostak[18] calculated the interaction energy of the linear helium trimer with the self-consistent LCAO method in 1955. The effect of nonadditive three-body forces on the third virial coefficient was estimated in 1966 by Sherwood, De Rocco, and Mason[19]. Novaro and Beltran-Lopez[20] tested the pairwise additivity in the helium trimer at short ranges by predicting the potential energy surface using SCF-LCAO-MO calculations in 1972. More recently, in 1993, Parish and Dykstra[21] carried out calculations at the coupled cluster level with double substitutions using very large basis sets to investigate the many-body contributions to interaction potentials and the second-order exchange-dispersion energy. In 1995, Røeggen and Almlöf[22] used an extended group function model for calculations of the three-body potential to obtain results more accurate than those previously available.

Several types of quantum Monte Carlo calculations have been reported earlier. In 1990, Mohan and Anderson[23] reported diffusion QMC calculations for the equilateral triangle configuration of the trimer. In 1992, Tawa *et al.*[24] reported variational QMC calculations of similar accuracies for triangular configurations. 'Exact' QMC calculations, without node location error, were reported by Bhattacharya and Anderson[25] for linear configurations. In the present work, diffusion Monte Carlo was used for both helium dimers and trimers.

The energies calculated are with respect to separated atoms. For clusters of more than two helium atoms, the energy can be thought of as consisting of two terms, the energy of the pairs of atoms and a multibody correction. Specifically, for a trimer:

$$
\begin{aligned}
\text{Monomer:} \quad & E_1 \\
\text{Dimer:} \quad & E_2 = \Sigma_2\, E_1 + \Delta E_2 \\
\text{Trimer:} \quad & E_3 = \Sigma_3\, E_1 + \Sigma_3\, \Delta E_2 + \Delta E_3
\end{aligned}
\tag{3.1}
$$

In this research, the energies of helium dimers and trimers relative to separated atoms were calculated, along with the correction to the pairwise-additive energy, ΔE_3.

Calculation Procedure

The calculations were carried out with the fixed-node diffusion quantum Monte Carlo (DQMC) method. For the dimer calculations, the trial function used was that due to Lowther and Coldwell[26] having the form:

$$
\psi_0 = \varphi_{A13}\varphi_{B24}e^{-\frac{U_{1324}}{2}} - \varphi_{A14}\varphi_{B23}e^{-\frac{U_{1423}}{2}} - \varphi_{A23}\varphi_{B14}e^{-\frac{U_{2314}}{2}} + \varphi_{A24}\varphi_{B13}e^{-\frac{U_{2413}}{2}}
\tag{3.2}
$$

where φ_{Nij} is a 189-term Hylleraas-like function and U_{ijkl} contains cross-terms for the electron-electron interactions, with A and B referring to the two helium nuclei and the numerals 1 through 4 referring to the four electrons. The trial function used for the trimer calculations was a similar 36-term function described by Bhattacharya and Anderson.[25] The calculations were run for internuclear distances of 4.5, 5.6, 6.5, and 7.5 bohr. For each geometry, calculations were run at three step sizes (0.010, 0.005, and 0.002 a.u.) and the results extrapolated to a step size of zero.

For comparison, calculations using the Gaussian 03 suite of programs were run. The methods used were Hartree-Fock (HF), fourth-order Møller-Plesset (MP4), and coupled-cluster at the single and doubles level (CCSD). The HF and CCSD calculations used the 6-311G** basis set; the MP4 calculations used the aug-cc-pV5Z basis set. Also calculated were the trimer energies predicted by the ATM expression:

$$\Delta E_3 = C \frac{3 \cos \gamma_1 \cos \gamma_2 \cos \gamma_3 + 1}{r_{12}^3 r_{23}^3 r_{31}^3} \tag{3.3}$$

where r_{12}, r_{23}, and r_{31} are the internuclear distances and γ_1, γ_2, and γ_3, are the included angles. C is a positive constant on the order $V\alpha^3$, where V is the ionization energy and α is the polarizability, having a value of 1.478 au, as given by Røeggen and Almlöf.[22] The Gaussian and ATM calculations were run for internuclear distances of 2.5, 3.5, 4.5, 5.6, 6.5, and 7.5 bohr.

Results

The potential energies for the helium dimer relative to the exact value for a pair of separated atoms were calculated for four internuclear distances between 4.5 and 7.5 bohr at three different time-steps: 0.002, 0.005, and 0.010 au. The data from the calculations for each distance are presented in Figures 3.1 through 3.4 and the results are listed in Table 3.1. The error bars in the graphs indicate 1σ statistical error in the points and the values in parentheses in the tables indicate 1σ statistical error in the last digit as determined from repeated calculations.

He$_2$ (R = 4.5 bohr)
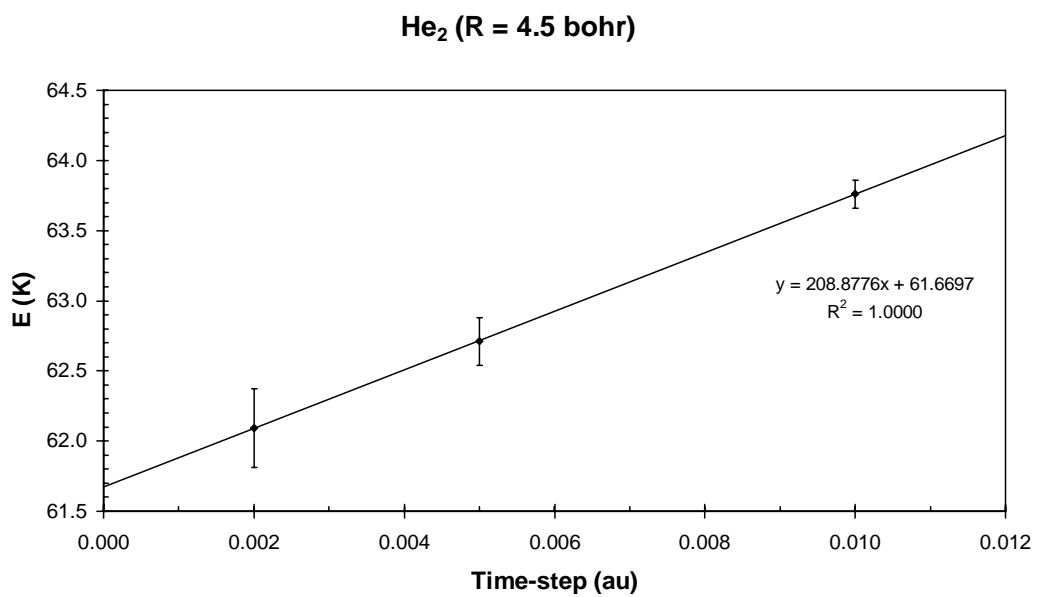
Figure 3.1 Calculated interaction energy ΔE_2 for the helium dimer at a distance of 4.5 bohr at three time-step sizes.

He$_2$ (R = 5.6 bohr)

y = 130.6408x - 10.9196
R^2 = 0.9984
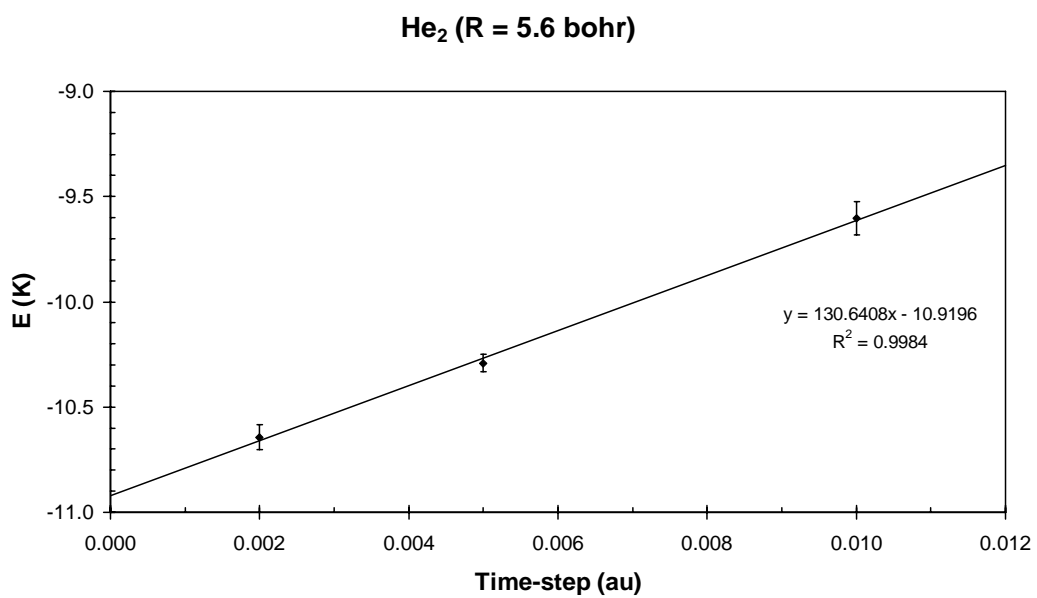
Figure 3.2 Calculated interaction energy ΔE$_2$ for the helium dimer at a distance of 5.6 bohr at three time-step sizes.

He$_2$ (R = 6.5 bohr)
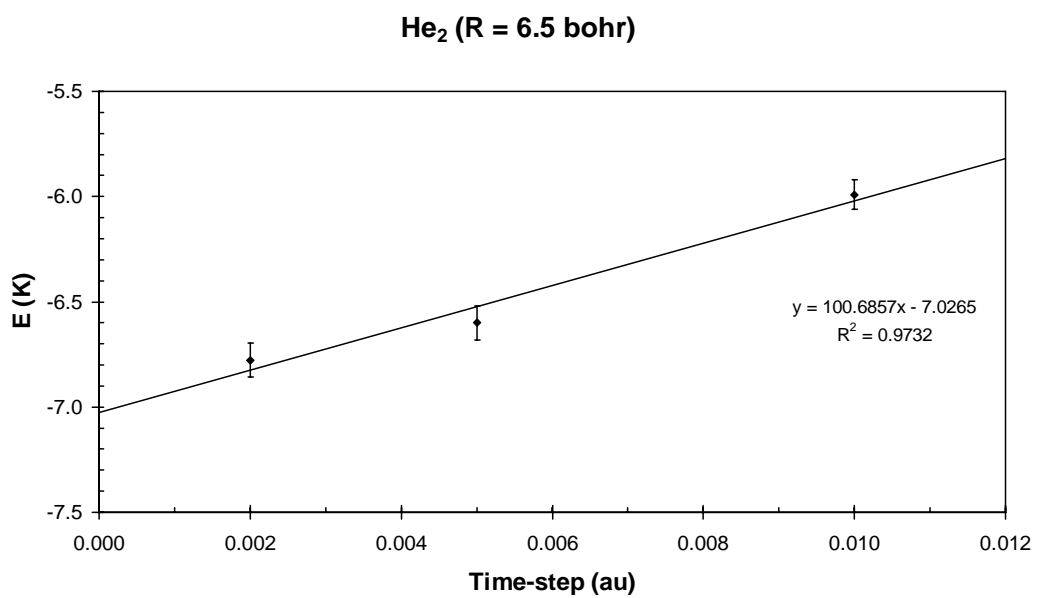
Figure 3.3 Calculated interaction energy ΔE$_2$ for the helium dimer at a distance of 6.5 bohr at three time-step sizes.

He$_2$ (R = 7.5 bohr)
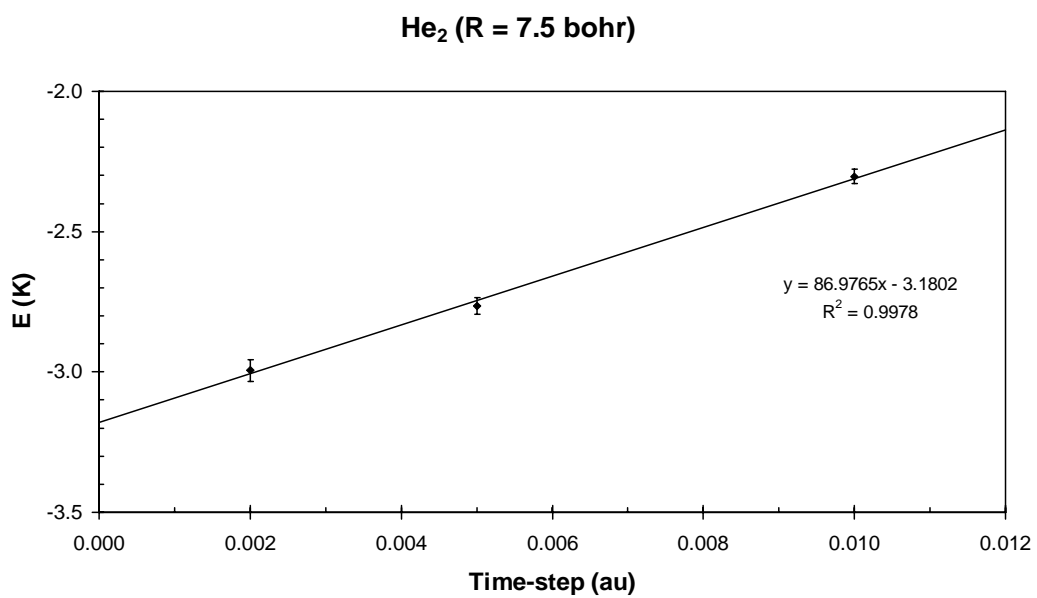
Figure 3.4 *Calculated interaction energy ΔE$_2$ for the helium dimer at a distance of 7.5 bohr at three time-step sizes.*

Table 3.1 Interaction energy calculated for the
helium dimer by the diffusion quantum Monte Carlo method.

| Internuclear distance | Interaction Energy ΔE_2 (K) | |
	Exact QMC[a]	DQMC (present work)
R (bohr)		
4.5	58.3(5)	61.7(4)
5.6	-10.998(5)	-10.92(8)
6.5	-6.930(5)[b]	-7.03(5)
7.5	-3.073(3)	-3.18(4)

[a]Reference 14
[b]Interpolated

The DQMC calculations for the equilateral triangle form of the helium trimer were calculated at the same four internuclear distances as the helium dimer and with the same time-steps. The data from the calculations for each distance are shown in Figures 3.5 through 3.8 and the results are listed in Table 3.2.

Figure 3.5 *Interaction energy for the helium trimer in equilateral triangle*
configuration with sides of 4.5 bohr at three time-step sizes
and the corresponding pairwise-additive energy.

Equilateral Triangle He$_3$ (R = 5.6 bohr)

y = 391.92x - 32.759
R^2 = 0.9984

y = 221.8357x - 32.5792
R^2 = 0.9846

E (K)

Time-step (au)

With multibody interaction
Pairwise additive
With multibody interaction
Pairwise additive

Figure 5.6 Interaction energy for the helium trimer in equilateral triangle
configuration with sides of 5.6 bohr at three time-step sizes
and the corresponding pairwise-additive energy.

27

Equilateral Triangle He$_3$ (R = 6.5 bohr)

$y = 302.06x - 21.079$
$R^2 = 0.9732$

$y = 155.2571x - 20.9467$
$R^2 = 0.9542$

With multibody interaction
Pairwise additive
With multibody interaction
Pairwise additive

E (K)

Time-step (au)

*Figure 5.7 Interaction energy for the helium trimer in equilateral triangle
configuration with sides of 6.5 bohr at three time-step sizes
and the corresponding pairwise-additive energy.*

Equilateral Triangle He$_3$ (R = 7.5 bohr)

Figure 5.8 Interaction energy for the helium trimer in equilateral triangle configuration with sides of 7.5 bohr at three time-step sizes and the corresponding pairwise-additive energy.

Table 3.2 Results for the diffusion quantum Monte Carlo calculations for the helium trimer with equilateral triangle configuration.

R (bohr)	E (a.u.)	$E - 3E_1$ (K)	ΔE_2 (K)	ΔE_3 (K) Present work	ΔE_3 (K) Mohan and Anderson[a]
2.5^a	-8.6062(5)	33190(160)	13040(60)		-5930(240)
3.5^a	-8.70088(13)	3260(40)	1169(30)		-247(100)
4.5	-8.7106058(15)	176.19(7)	61.7(4)	-8.8(12)	-4(30)
5.6	-8.7112727(6)	-32.58(17)	-10.92(8)	0.2(4)	1(10)
6.5	-8.7112395(3)	-20.95(14)	-7.03(5)	0.13(28)	-9(10)
7.5	-8.71120211(19)	-9.15(6)	-3.18(4)	0.39(18)	

[a]Reference 23

The DQMC calculations for the symmetric linear form of the helium trimer were calculated at the same four internuclear distances as the helium dimer and with the same time-step sizes. The data from the calculations for each distance are shown in Figures 3.9 through 3.12 and the results are listed in Table 3.3.

Linear He$_3$ (R = 4.5 bohr)

y = 517.76x + 122.35
R^2 = 1

y = 378.6735x + 122.7142
R^2 = 0.9920

With multibody interaction
Pairwise additive
With multibody interaction
Pairwise additive

E (K)
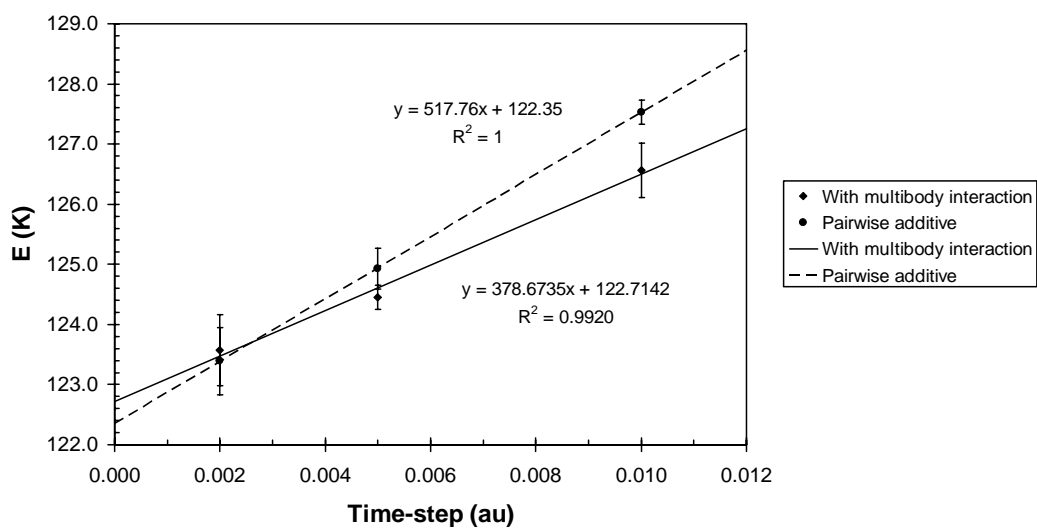
Time-step (au)

Figure 3.9 Interaction energy for the helium trimer in symmetric linear configuration with sides of 4.5 bohr at three time-step sizes and the corresponding pairwise-additive energy.

Linear He₃ (R = 5.6 bohr)

$y = 361.28x - 22.131$
$R^2 = 0.9991$

$y = 221.2755x - 21.7398$
$R^2 = 1.0000$

- ♦ With multibody interaction
- ● Pairwise additive
- —— With multibody interaction
- – – Pairwise additive
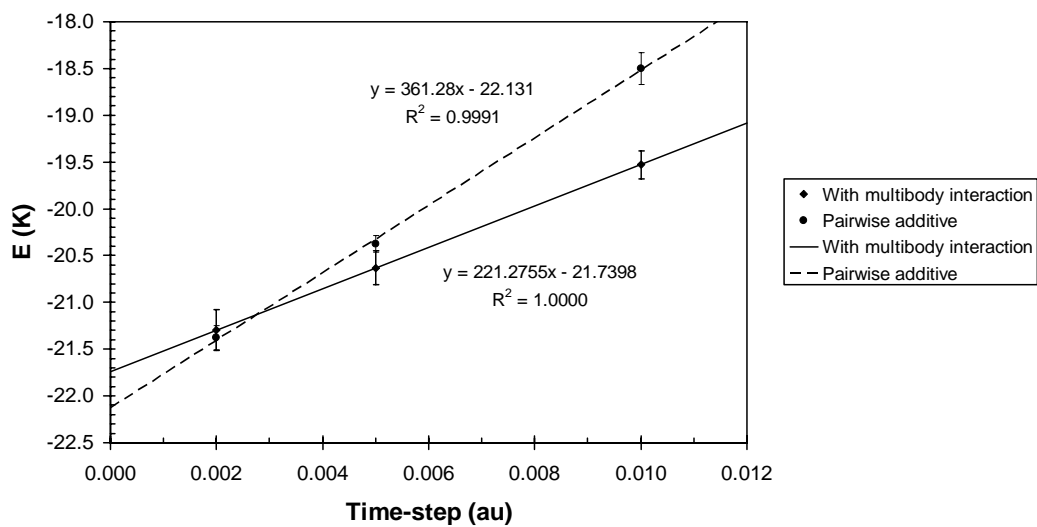
Figure 3.10 Interaction energy for the helium trimer in symmetric linear configuration with sides of 5.6 bohr at three time-step sizes and the corresponding pairwise-additive energy.

Linear He$_3$ (R = 6.5 bohr)

y = 301.37x - 14.178
R^2 = 0.9879

y = 67.6555x - 13.1400
R^2 = 0.8752

E (K)

Time-step (au)

With multibody interaction
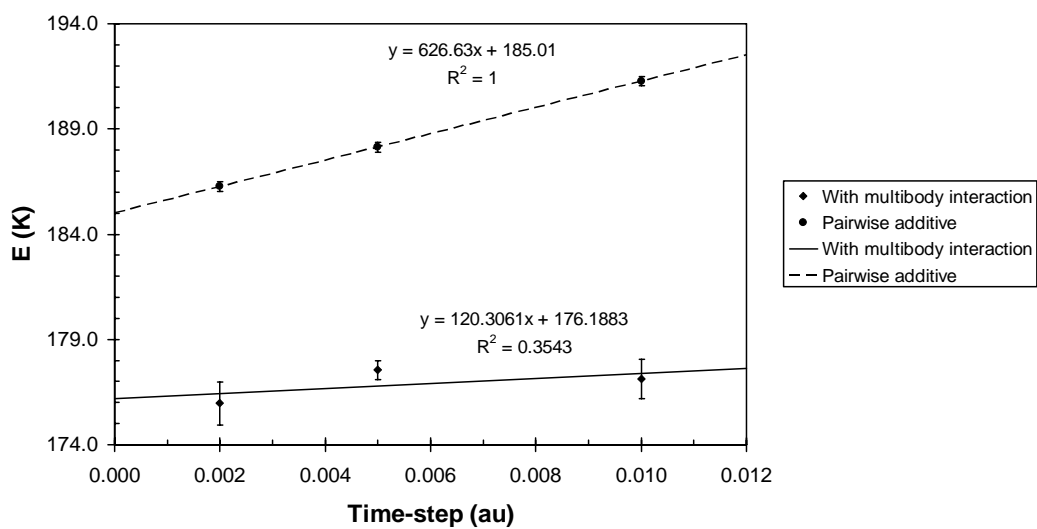Pairwise additive
With multibody interaction
Pairwise additive
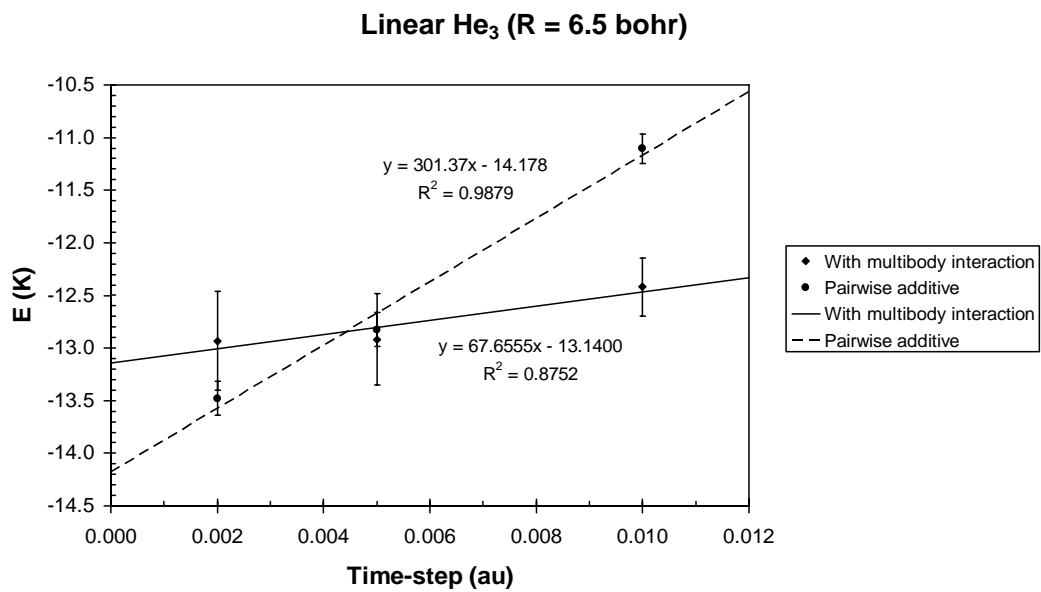
Figure 3.11 Interaction energy for the helium trimer in symmetric linear configuration with sides of 6.5 bohr at three time-step sizes and the corresponding pairwise-additive energy.

Linear He$_3$ (R = 7.5 bohr)

$y = 273.95x - 6.4028$
$R^2 = 0.9991$

$y = 137.9316x - 6.4349$
$R^2 = 0.9870$

With multibody interaction
Pairwise additive
With multibody interaction
Pairwise additive

E (K)
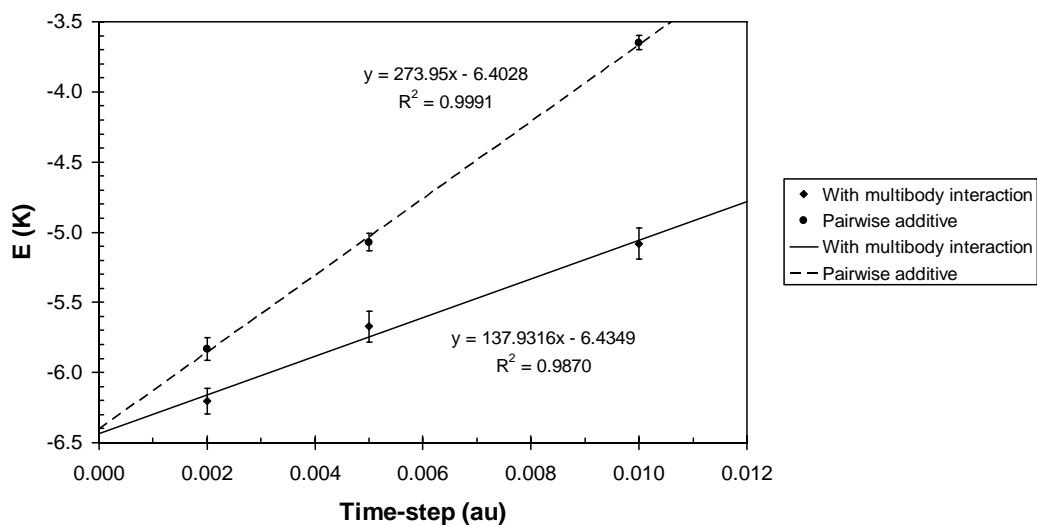
Time-step (au)

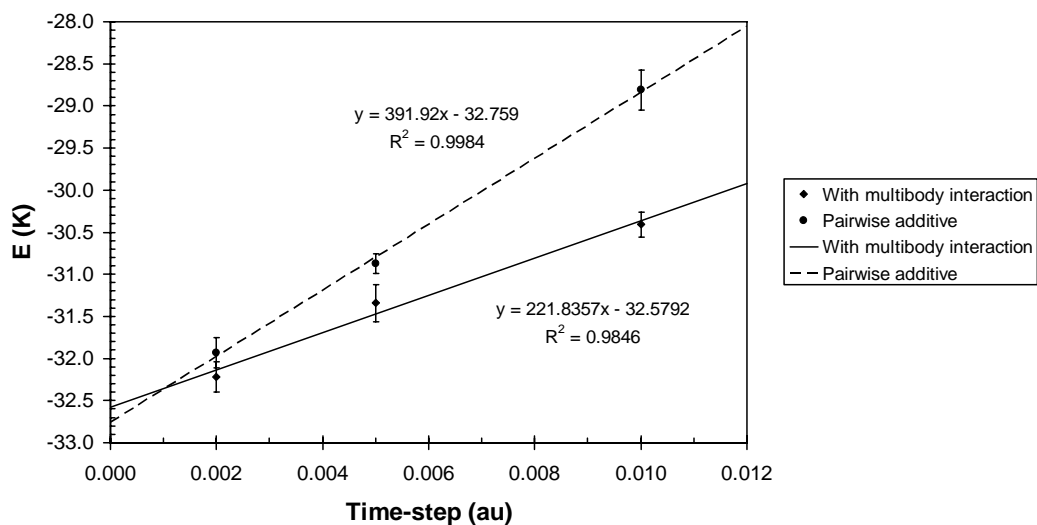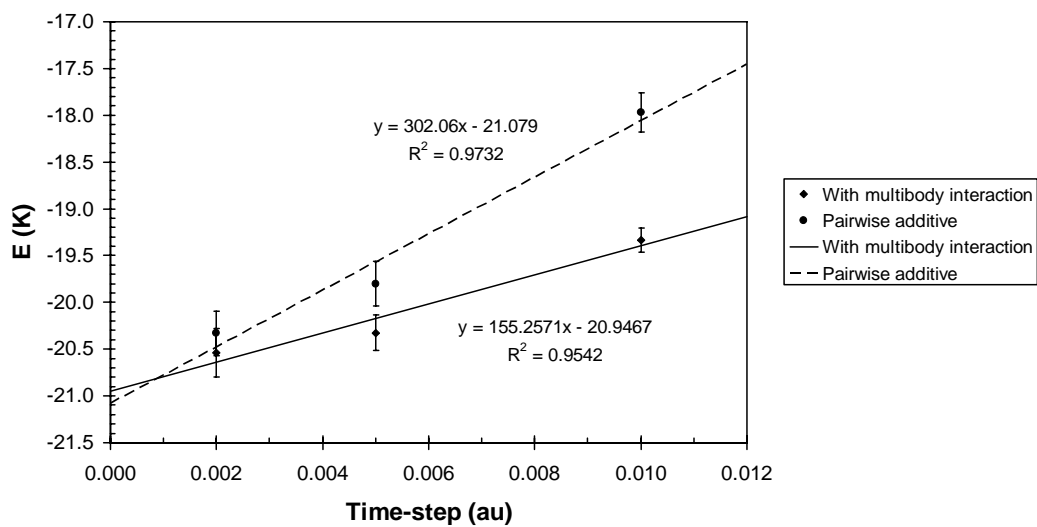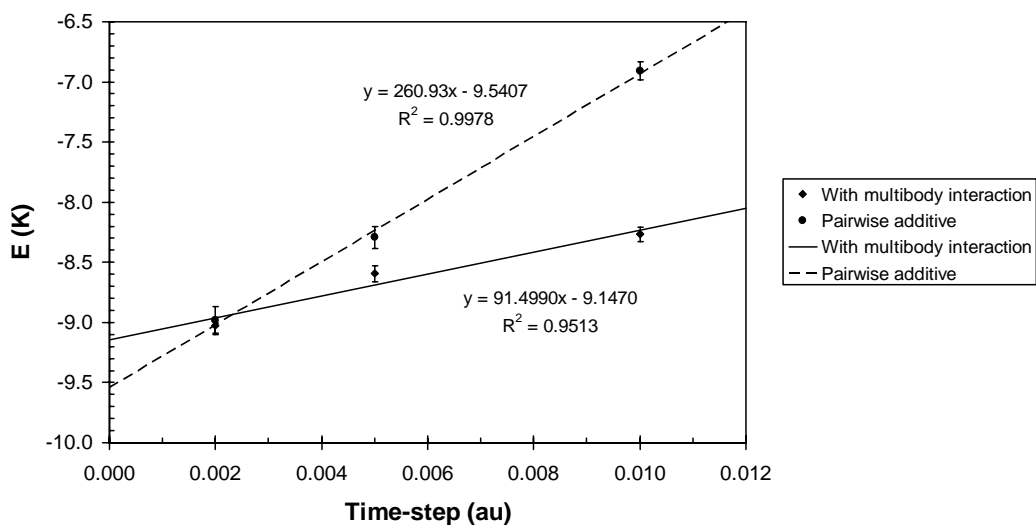*Figure 3.12 Interaction energy for the helium trimer in symmetric linear configuration with sides of 7.5 bohr at three time-step sizes and the corresponding pairwise-additive energy.*

Table 3.3 Results for the diffusion quantum Monte Carlo calculations for the helium trimer with symmetric linear configuration.

R (bohr)	E (a.u.)	$E - 3E_1$ (K)	ΔE_2 (K)	ΔE_3 (K) Present work	ΔE_3 (K) Bhattacharya and Anderson[a]
3.5^a	-8.70417(19)	2200(60)	2225(7)		-20(70)
4.5	-8.7107846(16)	122.7(5)	61.7(4)	0.4(12)	-13(12)
5.6	-8.7112418(10)	-21.7(3)	-10.92(8)	0.3(5)	0.7(21)
6.5	-8.7112146(19)	-13.1(6)	-7.03(5)	1.0(7)	0.8(13)
7.5	-8.71119349(29)	-6.43(9)	-3.18(4)	-0.03(18)	

[a]Reference 25

The results of the Gaussian 03 calculations and the ATM three-body correction term for six interatomic distances between 2.5 and 7.5 bohr are listed in Table 3.4 for the equilateral triangle geometry and Table 3.5 for the symmetric linear geometry.

Table 3.4 Correction to the pairwise-additive energy calculated for helium trimers in an equilateral triangle geometry by various methods.

R	Three-body Interaction Energy ΔE_3 (K)					
(bohr)	HF	CCSD	MP4	ATM	EGFM[a]	DQMC
2.5	-5708.46	-5902.54	-5610.95	168.32		-5930(240)[b]
3.5	-284.26	-317.42	-288.90	8.15	-285	-274(100)[b]
4.5	-7.67	-9.13	-10.70	0.85	-9.8	-8.8(12)
5.6	0.22	0.19	-0.25	0.12	-0.05	0.2(4)
6.5	0.06	0.06	-0.03	0.03	0.04	0.13(28)
7.5	0.00	0.09	0.03	0.01	0.01	0.39(18)

[a]Reference 22
[b]Reference 23

Table 3.5 Correction to the pairwise-additive energy calculated for helium trimers in a symmetric linear geometry by various methods.

R	Three-body Interaction Energy ΔE_3 (K)					
(bohr)	HF	CCSD	MP4	ATM	EGFM[a]	DQMC
2.5	601.58	638.05	638.53	-30.60		
3.5	11.87	12.28	13.39	-1.48	16.2	-20(70)[b]
4.5	0.03	-0.3	-0.13	-0.15	0.26	0.4(12)
5.6	0.03	0.0	-0.03	-0.02	-0.010	0.3(5)
6.5	0.03	0.3	-0.06	-0.01	-0.005	1.0(7)
7.5	0.00	0.1	0.00	0.00	-0.001	-0.03(18)

[a]Reference 22
[b]Reference 25

Discussion

The results of our calculations are in good agreement with previous quantum Monte Carlo calculations. We have reduced the statistical errors in the quantum Monte Carlo calculations of the equilateral triangle helium trimer by Mohan and Anderson[23] by more than a factor of ten. The errors in the quantum Monte Carlo calculations of Bhattacharya and Anderson[25] of the symmetric linear geometry of the helium trimer were reduced by factors of two to ten. The reason for the improvement of the statistical errors is due both to using an improved trial function, incorporating a 189-term Hylleraas-like function as opposed to a 99-term one, and the general increase in computational power since the times the previous calculations were run. We find again that the three-body interaction of helium trimers in both configurations is very small for internuclear distances of 5.6 bohr and larger. We also find again that the ATM expression fails badly for internuclear distances of less than 4.5 bohr, and for the equilateral triangle, even the sign is wrong. An explanation for this is given by the analysis of Bulski and Chalasiński,[27] where the three-body correction is split into three contributions, of which the ATM expression is only a fraction of one, and the other two predominate at close distances. For internuclear distances of 5.6 bohr and greater, both the DQMC and the ATM values are both small, but the statistical error in the DQMC values prevents further comparisons.

The DQMC results are entirely compatible with the extended group function model (EGFM) results of Røeggen and Almlöf.[22] This is particularly evident for the smaller internuclear distances of the triangular case. In all cases,

the DQMC values fall within one or two standard deviations of the EGFM values. In this sense, the DQMC calculations confirm the EGFM results.

For the smaller internuclear distances, the several standard types of calculations (HF, CCSD, and MP4) give remarkably good agreement with each other and with the DQMC calculations for the three-body corrections despite poor values for the two-body interactions. This was observed in the earlier DQMC calculations.[23,25]

In one of the first calculations to use accurate pair potentials of the properties of liquid helium, Kalos *et al.*[28] found that predictions gave better agreement with experiment when the ATM correction was omitted than when it was included. Since then, a number of other calculations have been made for solid and liquid helium (^{3}He and ^{4}He) using several different three-body correction terms, some good and some bad, but most without any three-body correction term.[29] Results of our current calculations, together with those of the best prior calculations, give consistent predictions of three-body corrections and should lead to more accurate first principle calculations of the properties of solid and liquid helium and helium clusters.

CHAPTER 4

NEON

Introduction

In order to initially test the VQMC correction scheme, it was applied to two systems, neon and a related system referred to as "pseudo"-neon. The "pseudo"-neon system can be thought of as the neon system with the electron-electron interactions removed. This system has the advantage of having an analytic solution, with which the outcome of the correction scheme can be compared. The neon system does not have an analytic solution, so it will be compared to the result of a DQMC calculation.

Boys and Handy used the method of transcorrelated wavefunctions in 1969 to calculate an accurate energy of the neon atom, reporting it as −128.959 hartree.[30] In 1976, Clary and Handy used a combined configuration-interaction − Hylleraas method to perform a variational calculation on the neon atom, resulting in a value for the energy of −128.8298 hartree for an 83-term wavefunction.[31] More recently, in 1990, Schmidt and Moskowitz reported the use of the variational Monte Carlo method to produce a wavefunction consisting of a self-consistent wavefunction multiplied by a Boys and Handy correlated wavefunction.[32] Their result was an energy of −128.8796(6) hartree. The experimental result was obtained by Hartmann and Clementi[33] in 1964, which they report as having a value of −128.929 hartree.

Calculation Procedure

The calculations were run using both the fixed-node diffusion and variational quantum Monte Carlo methods. The trial wavefunction for neon used in the QMC calculations is reproduced from Schmidt and Moskowitz[32]:

$$\psi_0 = F\Phi$$

$$F = \exp\sum_{i<j} U_{ij}$$

$$U_{ij} = \sum_{k}^{17} \Delta(m_k, n_k) c_k (\overline{r}_{iX}^{m_k} \overline{r}_{jX}^{n_k} + \overline{r}_{jX}^{m_k} \overline{r}_{iX}^{n_k}) \overline{r}_{ij}^{o_k}$$

$$\overline{r}_{iX} = \frac{r_{iX}}{1 + r_{iX}}$$

$$\overline{r}_{ij} = \frac{r_{ij}}{1 + r_{ij}}$$

(4.1)

where F is a product of electron-electron and electron-electron-nucleus correlations, i and j indicate electrons, X indicates the nucleus, r_{ab} is the distance between a and b, m, n, and o are taken to be integers, and Φ is a product of an up-spin determinant and a down-spin determinant. The trial wavefunction used for 'pseudo'-neon has the electron-electron interactions removed. The DQMC calculations were run for 1×10^6 steps with 2000 walkers at time-steps of 1×10^{-5}, 5×10^{-5}, and 1×10^{-4} au. The VQMC calculations were run for 5×10^8 steps, with the correction calculations run for 5×10^5 steps with 440 walkers at time-steps of 1×10^{-5}, 5×10^{-5}, and 1×10^{-4} au.

Results

       The data from the calculations of 'pseudo'-neon are presented in Figure 4.1 and the data for neon in Figure 4.2. The error bars indicate 1σ statistical error as determined from repeated calculations. Table 4.1 shows the calculated terms for the correction to the VQMC energy along with the VQMC, corrected VQMC, and DQMC results.
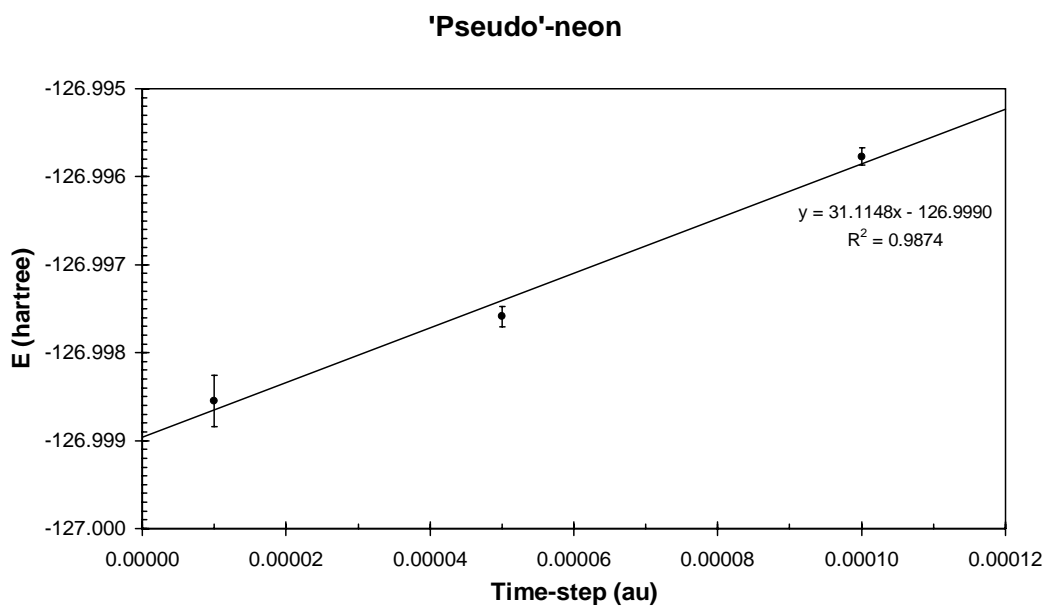
'Pseudo'-neon

Figure 4.1 Calculated DQMC energy for 'pseudo'-neon at three time-step sizes.
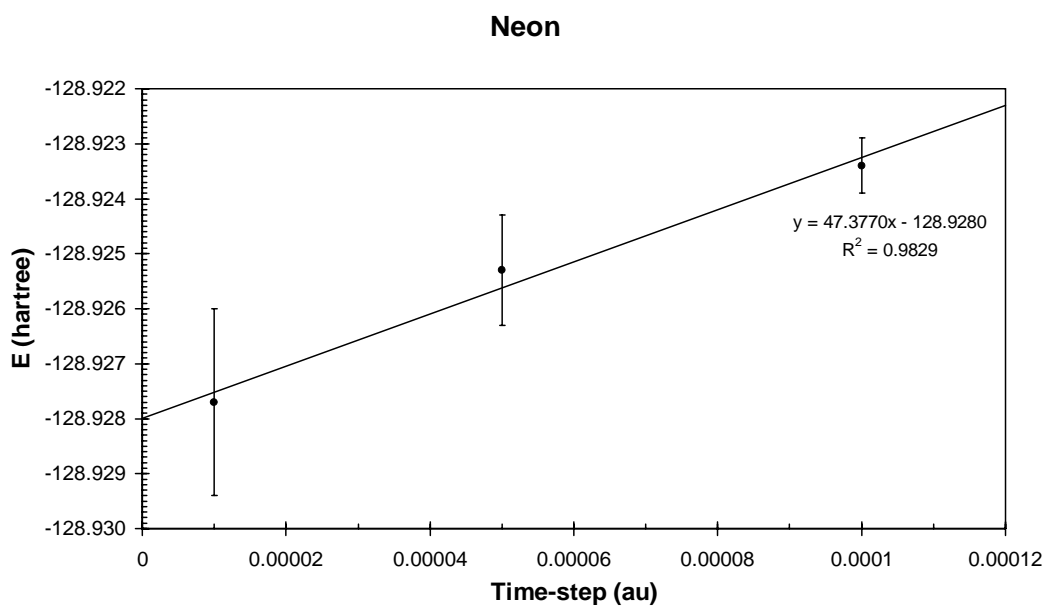
Figure 4.2 Calculated DQMC energy for neon at three time-step sizes.

**Table 4.1 Terms in the correction factor for the VQMC
energy of 'pseudo'-neon and neon and comparison energies.**

	'Pseudo'-neon	Neon
I_n/I_q	0.4785(4)	0.542(6)
I_p/I_q	-0.4785(5)	-0.541(8)
f_n	0.979(6)	0.925(5)
f_p	1.083(7)	1.032(4)
f_q	1.030(6)	0.993(4)
Correction (hartree)	0.048(4)	0.059(4)
VQMC Energy (hartree)	-126.94974(8)	-128.8678(13)
VQMC Energy – Correction (hartree)	-126.998(4)	-128.926(4)
DQMC Energy (hartree)	-126.9990(3)	-129.9280(20)
Analytic Solution (hartree)	-127	

Discussion

It is apparent that the correction scheme works well in bringing the VQMC energy for both 'pseudo'-neon and neon very close to the DQMC value. For 'pseudo'-neon, the correction scheme makes up 98% of the difference between the VQMC and DQMC energies and 96% of the difference between the VQMC and analytic energies. For neon, the correction scheme makes up 97% of the difference between the VQMC and DQMC energies. As a test case, these results are very promising and show that this correction scheme has the potential to work nearly as well as DQMC, with the added benefit that the uncertainly due to time step error is restricted to the correction portion of the calculation, since the bulk of the energy comes from the VQMC step, rather than the entire calculation, as in DQMC.

CHAPTER 5

DIATOMIC HYDROGEN

Introduction

QMC calculations were run for diatomic hydrogen for the purpose of investigating the application of the correction scheme to a well known system, for which nearly exact solutions are known. This system allows for accurate and short DQMC calculations to be run as a comparison to the VQMC and correction calculations over a number of points on the potential energy curve.

The first calculation of the expectation value of the binding energy of diatomic hydrogen was done by Heitler and London in 1927.[34] Their calculations resulted in a binding energy of 3.20 eV (0.118 hartree) at an internuclear distance of 0.80 Å (1.5 bohr). Coulson calculated a binding energy of 3.488 eV (0.1282 hartree) at 0.732 Å (1.38 bohr) in 1937 using a product of two H_2^+-like molecular orbitals.[35] Shull and Hagstrom used a single-center Laguerre function at the center of the H_2 molecule with 44 configurations to obtain a value of 4.3920 eV (0.16141 hartree) for the binding energy at 1.4 bohr in 1959.[36] The experimental value of the binding energy was determined in 1957 by Shoicheff to be 4.746 eV (0.1744 hartree) at a distance of 1.4008 bohr.[37]

More recently, in 1993, Wolniewicz calculated the ground state energy to be −1.174475671 hartree.[38] The most recent, highly accurate value for the energy of H_2 was obtained in 2006 by Sims and Hagstrom.[39] They reported a ground

state energy of $-1.174475714220(1)$ hartree at an internuclear distance of 1.4 bohr, using Hylleraas variational calculations with 7034 expansion terms.

Calculation Procedure

The calculations were carried out with both the fixed-node diffusion and variational quantum Monte Carlo methods. The trial wavefunction, ψ_0, used for the calculations was:

$$\psi_0 = \left(e^{-1.197r_{1A}} + e^{-1.197r_{1B}}\right)\left(e^{-1.197r_{2A}} + e^{-1.197r_{2B}}\right)e^{\frac{0.5r_{12}}{1+r_{12}}} \qquad (5.1)$$

where r_{nX} is the distance between electron n and nucleus X, and r_{12} is the distance between the two electrons. The first two terms are each an H_2^+-like molecular orbital, one for each electron. The third term is a simple Jastrow function, which adds electron interaction to the wavefunction. The constant in the exponent was determined by Coulson in his variational calculation.[35] The calculations were run for internuclear distances of 1.0 bohr to 2.1 bohr, incremented by 0.1 bohr. The DQMC calculations were run with 1000 walkers for 1×10^5 steps using step sizes of 1×10^{-3}, 2×10^{-3}, and 5×10^{-3} au and the correction to the VQMC calculations with 1000 walkers for 2×10^4 steps using step sizes of 1×10^{-4}, 2×10^{-4}, and 5×10^{-4}, with the results of both extrapolated to a step size of zero. The VQMC calculations were run for 1×10^9 steps.

Results

The DQMC simulations took approximately sixty hours to run at each point, while both the VQMC and the correction calculations each took approximately 10 hours. The terms for the correction to the VQMC energy of H_2 at each of the internuclear distances (R) are displayed in Table 5.1, along with the calculated correction value, using Equation 2.9. The results of the DQMC and VQMC calculations for H_2 at various internuclear distances are given in Table 5.2, along with the corrected VQMC energies. The uncertainties in the values indicate 1σ statistical error as determined from repeated calculations. A graphical comparison of the calculated DQMC, VQMC, and corrected VQMC energies is shown in Figure 5.1. Also included in the graph are the results obtained by Sims and Hagstrom from Hylleraas variational calculations.[39]

Table 5.1 Terms in the correction factor for the VQMC energy of H$_2$ at various internuclear distances.

R (bohr)	I$_n$/I$_q$	I$_p$/I$_q$	f$_n$	f$_p$	f$_q$	Correction (hartree)
1.0	-0.132045	0.132045	0.873676	1.209755	1.039974	0.04267
1.1	-0.119188	0.119187	0.883433	1.165597	1.033008	0.03255
1.2	-0.108848	0.108848	0.888392	1.1456	1.028905	0.02721
1.3	-0.101003	0.101003	0.876515	1.138769	1.023875	0.02587
1.4	-0.095679	0.095679	0.870123	1.12657	1.022598	0.02399
1.5	-0.092922	0.092922	0.860836	1.124868	1.02193	0.02400
1.6	-0.092197	0.092197	0.852569	1.127887	1.022386	0.02482
1.7	-0.093062	0.093062	0.82943	1.122128	1.025179	0.02657
1.8	-0.095131	0.095131	0.830616	1.123442	1.028346	0.02708
1.9	-0.098178	0.098178	0.815585	1.125086	1.033197	0.02940
2.0	-0.101890	0.101890	0.798954	1.143179	1.036304	0.03384
2.1	-0.105978	0.105977	0.797626	1.143219	1.039522	0.03523

Table 5.2 DQMC, VQMC, and corrected VQMC energies for H$_2$ at various internuclear distances.

R (bohr)	DQMC Energy (hartree)	VQMC Energy (hartree)	VQMC Energy – Correction (hartree)
1.0	-1.1247(26)	-1.07982(29)	-1.12249
1.1	-1.1509(24)	-1.11322(27)	-1.14577
1.2	-1.1650(11)	-1.13349(25)	-1.16070
1.3	-1.1730(7)	-1.14420(24)	-1.17007
1.4	-1.1746(7)	-1.14797(23)	-1.17197
1.5	-1.1736(29)	-1.14647(24)	-1.17048
1.6	-1.1690(25)	-1.14117(24)	-1.16600
1.7	-1.1625(20)	-1.13299(25)	-1.15956
1.8	-1.1549(13)	-1.12276(27)	-1.14985
1.9	-1.1472(14)	-1.11098(29)	-1.14039
2.0	-1.1382(5)	-1.0982(3)	-1.13200
2.1	-1.1291(4)	-1.0845(3)	-1.11970

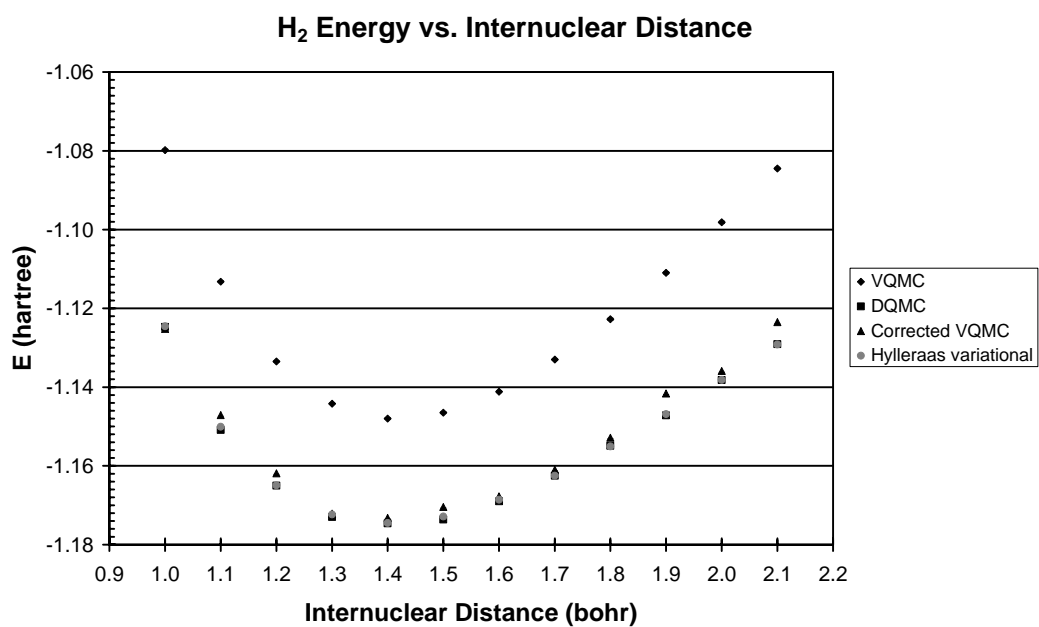**H₂ Energy vs. Internuclear Distance**

Figure 5.1 H₂ energy for various internuclear distances using VQMC and DQMC methods, along with the corrected VQMC and Hylleraas variational values.

Discussion

The DQMC calculations give the best result, resulting in the lowest energy at all internuclear distances. Converting the value of $-1.1746(7)$ hartree at 1.4 bohr to binding energy by comparing to the energy of two individual hydrogen atoms (-0.5 hartree each) gives $0.1746(7)$ hartree, which is in very good agreement with the experimental value of 0.1744 hartree. This ground state energy at 1.4 bohr is also in agreement with the most accurate value obtained by Sims and Hagstrom of $-1.174475714220(1)$ hartree.[39] The VQMC calculations are higher than the DQMC value by approximately 0.03 to 0.04 hartree, with the deviation increasing with the displacement of the internuclear distance from the minimum energy value of 1.4 bohr. As seen in Figure 5.1, the corrected VQMC energy is almost as good as the DQMC value.

The time it took to obtain a value from the DQMC calculation for a given internuclear distance with a certain uncertainty was approximately twice as long as the combined time for the VQMC calculation and the correction calculation with the same uncertainty. These results show promise that running this correction scheme for a VQMC calculation of a more complicated molecule will be nearly as good as a DQMC calculation having the same uncertainty, without taking as much computational power. Since these calculations scale as the third power of the number of electrons in the system, the benefit from this correction scheme will be more apparent for systems of much larger size, in which the time savings outweighs the fact that this method does not quite do as well as DQMC.

CHAPTER 5

C$_{10}$

Introduction

Carbon clusters have significance in various natural processes. In astrophysics, they are contributors to the formation of carbon dust, polycyclic aromatic hydrocarbons, and diffuse interstellar bands. Also, the formation of soot in hydrocarbon flames is started by large carbon clusters.[40] These carbon clusters are able to form in many different geometrical structures, such as chains, rings, fused rings, and cages. The difference in energy between the most stable forms of a given cluster can be very small. Because of this, it is hard to determine which geometry is actually the most stable, and in general, different methods of predicting relative energies give varying results.

One of the earliest calculations on C$_{10}$ was by Bernholc and Phillips[41] in 1986. They used self-consistent modified neglect of differential overlap calculations for carbon clusters ranging from C$_1$ to C$_{26}$, and reported several carbon clusters with maximum stabilities, one of which was C$_{10}$. In 1987, Raghavachari and Binkley[42] used the Hartree-Fock method to determine the molecular geometry of C$_{10}$ as nearly a pentagon, with alternating bond angles of 119.4° and 168.6° and a bond distance of 1.290 Å. They then calculated the energy with fourth-order Møller-Plesset perturbation theory, obtaining a value of –379.59768 hartree. Liang and Schaefer[43] studied the structure of C$_{10}$ using the configuration interaction method in 1990. They looked at five structures, three

52

monocyclic rings and two linear structures. Their conclusion was that all the monocyclic structures were more stable than the linear ones, with the most stable structure having a similar geometry to that of Raghavachari and Binkley: alternating bond angles of 118.9° and 169.1° with a bond length of 1.295 Å. Its energy was calculated to be –379.17948 hartree. In 1995, Martin and Taylor[44] reported an energy of –379.926126 hartree for a distorted cyclic C_{10} structure with all equal bond lengths using a couple-cluster method. In 1995, Grossman, Miras, and Raghavachari[45], using a diffusion quantum Monte Carlo approach, found the geometry with all bond angles of 144° and alternating bond lengths to be the lowest in energy, 0.3(1) eV less than the regular decagon structure. In 1999, Shlyakhter, Sokolova, Lüchow, and Anderson[46] used fixed-node diffusion quantum Monte Carlo calculations on four structures: one linear and three monocyclic. They reported the lowest energy structure to be a regular decagon with bond lengths of 1.312 Å, having an energy of –380.413(6) hartree.

Calculation Procedure

The quantum Monte Carlo calculations for C_{10} were carried out with different ring sizes for geometries in which either the bond angles were alternated, or the bond lengths. The ring sizes were designated by their radii, and five different sizes were investigated: 2.04 Å, 2.08 Å, 2.12 Å, 2.16 Å, and 2.20 Å. For the alternating bond angle structures, the pairs of angles at which calculations were run were: (144°,144°), (148°,140°), (152°,136°), (156°,132°), (160°,128°), (164°,124°), and (176°,112°). Throughout this chapter the pairs are referred to by

their larger angle. For the alternating bond lengths, the calculations were run for different ratios of larger to smaller bond lengths, all with bond angles of 144°. The trial wavefunctions were single-determinant SCF functions multiplied by ten-term Schmidt-Moskowitz Jastrow functions, which introduce electron correlation. The SCF functions were obtained from GAUSSIAN[47] and GAMESS[48] calculations. As comparison, the SCF and MP4 energies were obtained from GAUSSIAN using the 6-31G** basis set.

<div align="center">

Results

</div>

The VQMC calculations took approximately 1200 hours to run at each point, while the correction calculations took approximately 900 hours. The results of the VQMC calculations in which all the bond lengths are equal and the bond angles are varied for different ring sizes can be found in Table 6.1. The corrections to these VQMC energies are shown in Table 6.2, with the resulting corrected energies in Table 6.3. The SCF and MP4 energies for comparison are given in Tables 6.4 and 6.5, respectively. Figures 6.1 through 6.7 display graphs comparing the VQMC and corrected VQMC energies for the five different ring radii at the seven bond angles, ranging from the least distorted ring to the greatest.

Table 6.1 VQMC energy of C$_{10}$
for various ring radii and alternating bond angles.

	2.04 Å	2.08 Å	2.12 Å	2.16 Å	2.20 Å
144°	-379.443(11)	-379.534(8)	-379.520(12)	-379.434(13)	-379.247(10)
148°	-379.474(9)	-379.555(9)	-379.457(13)	-379.385(12)	-379.352(12)
152°	-379.390(12)	-379.386(10)	-379.422(9)	-379.421(15)	-379.314(11)
156°	-379.371(10)	-379.421(11)	-379.456(9)	-379.363(10)	-379.310(10)
160°	-379.374(11)	-379.527(11)	-379.567(10)	-379.387(10)	-379.327(10)
164°	-379.432(11)	-379.505(17)	-379.568(12)	-379.459(11)	-379.348(9)
176°	-379.329(13)	-379.354(10)	-379.489(11)	-379.430(12)	-379.396(10)

Table 6.2 Correction to the VQMC energy of C$_{10}$
for various ring radii and alternating bond angles.

	2.04 Å	2.08 Å	2.12 Å	2.16 Å	2.20 Å
144°	0.9445	0.8012	0.7395	0.5127	0.5577
148°	0.8428	0.6496	0.4881	0.5045	0.4736
152°	0.5197	0.8339	0.8023	0.5962	0.4067
156°	0.4568	0.6120	0.6452	0.8067	0.8237
160°	0.5244	0.5039	0.7448	0.7908	0.8020
164°	0.4954	0.6156	0.6545	0.7090	0.7589
176°	0.3394	0.4870	0.6691	0.7301	0.6987

Table 6.3 Corrected VQMC energy of C$_{10}$
for various ring radii and alternating bond angles.

	2.04 Å	2.08 Å	2.12 Å	2.16 Å	2.20 Å
144°	-380.387(11)	-380.334(8)	-380.260(12)	-379.947(13)	-379.805(10)
148°	-380.316(9)	-380.205(9)	-379.945(13)	-379.885(12)	-379.825(12)
152°	-379.910(12)	-380.220(10)	-380.242(9)	-380.017(15)	-379.721(11)
156°	-379.828(10)	-380.033(11)	-380.101(9)	-380.163(10)	-380.134(10)
160°	-379.898(11)	-380.031(11)	-380.312(10)	-380.177(10)	-380.129(10)
164°	-379.927(11)	-380.121(17)	-380.222(12)	-380.159(11)	-380.107(9)
176°	-379.668(13)	-379.841(10)	-380.158(11)	-380.160(12)	-380.094(10)

Table 6.4 SCF energy of C_{10}
for various ring radii and alternating bond angles.

	2.04 Å	2.08 Å	2.12 Å	2.16 Å	2.20 Å
144°	-378.258	-378.257	-378.238	-378.203	-378.154
148°	-378.262	-378.263	-378.245	-378.212	-378.165
152°	-378.273	-378.275	-378.259	-378.227	-378.182
156°	-378.284	-378.287	-378.273	-378.244	-378.201
160°	-378.293	-378.298	-378.286	-378.259	-378.219
164°	-378.299	-378.306	-378.296	-378.271	-378.234
176°	-378.282	-378.298	-378.297	-378.281	-378.252

Table 6.5 MP4 energy of C_{10}
for various ring radii and alternating bond angles.

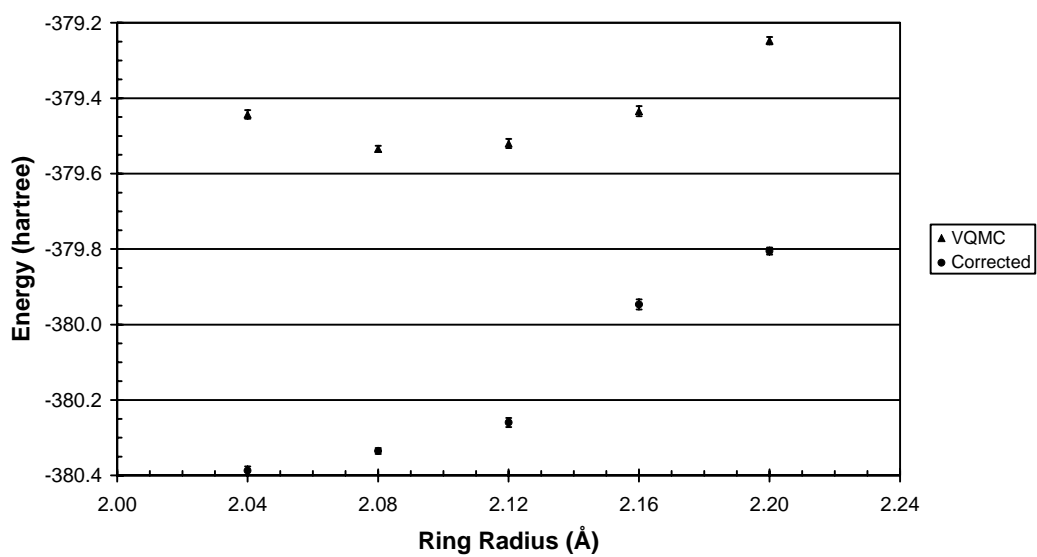|	2.04 Å	2.08 Å	2.12 Å	2.16 Å	2.20 Å
144°	-379.739	-379.762	-379.769	-379.761	-379.741
148°	-379.728	-379.749	-379.750	-379.734	-379.703
152°	-379.717	-379.735	-379.734	-379.717	-379.686
156°	-379.709	-379.727	-379.727	-379.710	-379.680
160°	-379.703	-379.723	-379.724	-379.709	-379.680
164°	-379.699	-379.720	-379.723	-379.710	-379.683
176°	-379.669	-379.699	-379.711	-379.707	-379.688

Alternating Bond Angles (144⁰,144⁰)

Figure 6.1 VQMC energy and corrected VQMC energy for C_{10} with bond angles of 144° for various ring radii.

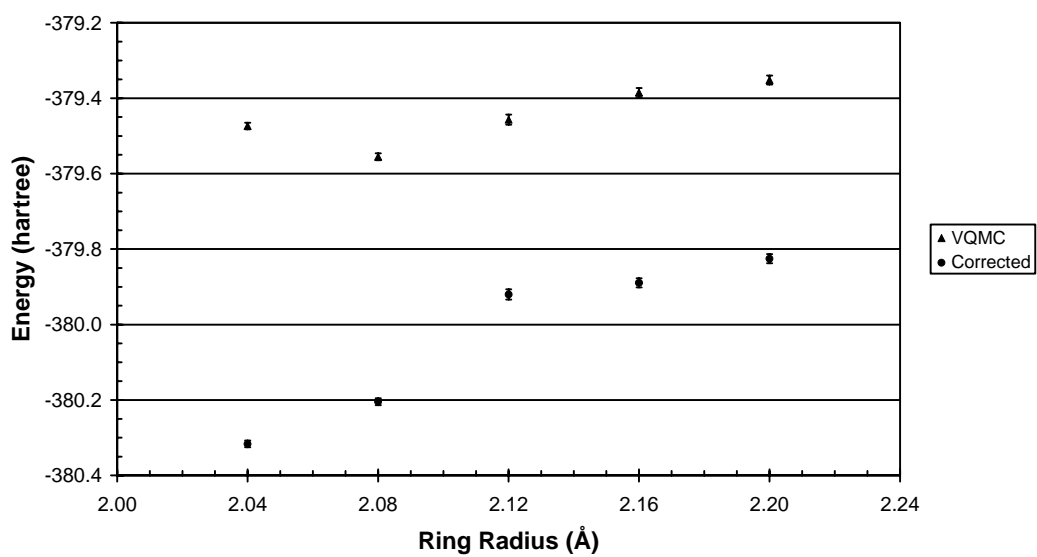**Alternating Bond Angles (140⁰,148⁰)**

Figure 6.2 VQMC energy and corrected VQMC energy for C_{10} with alternating bond angles of 148° and 140° for various ring radii.

Alternating Bond Angles (136⁰,152⁰)

Figure 6.3 VQMC energy and corrected VQMC energy for C_{10} with alternating bond angles of 152° and 136° for various ring radii.

Alternating Bond Angles (132⁰,156⁰)
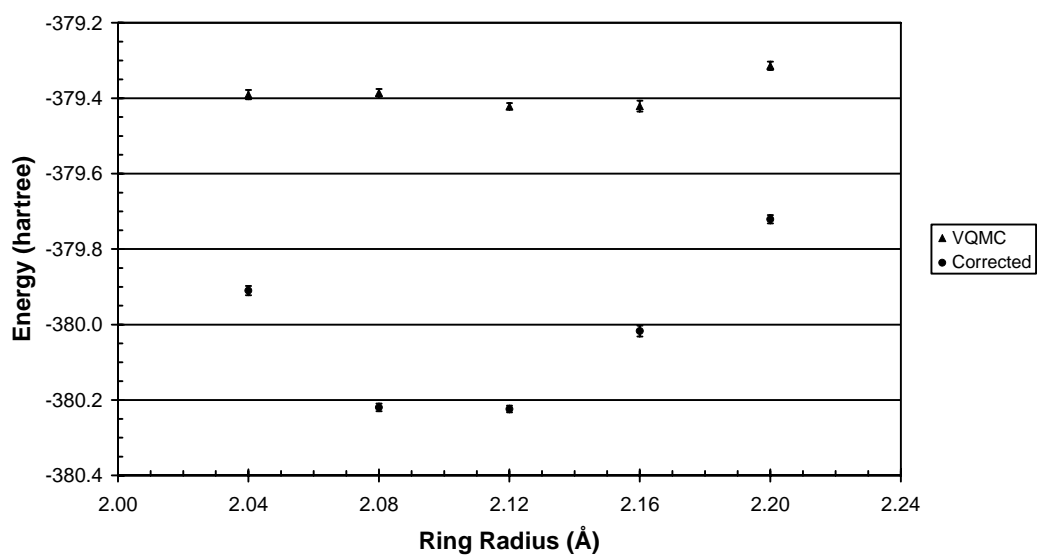

Figure 6.4 VQMC energy and corrected VQMC energy for C_{10} with alternating bond angles of 156° and 132° for various ring radii.

Alternating Bond Angles (128⁰,160⁰)
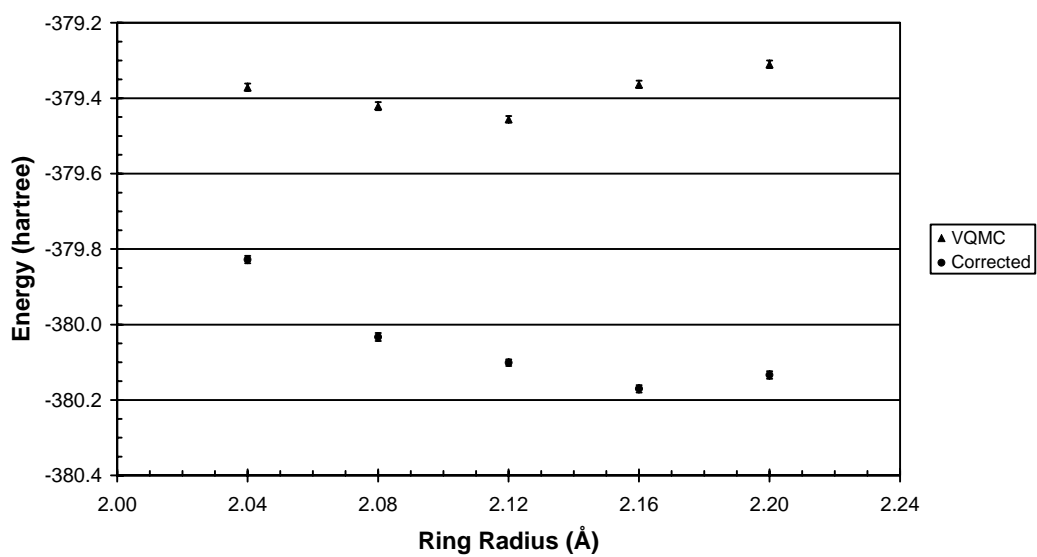

Figure 6.5 VQMC energy and corrected VQMC energy for C_{10} with alternating bond angles of 160° and 128° for various ring radii.

Alternating Bond Angles (124⁰,164⁰)
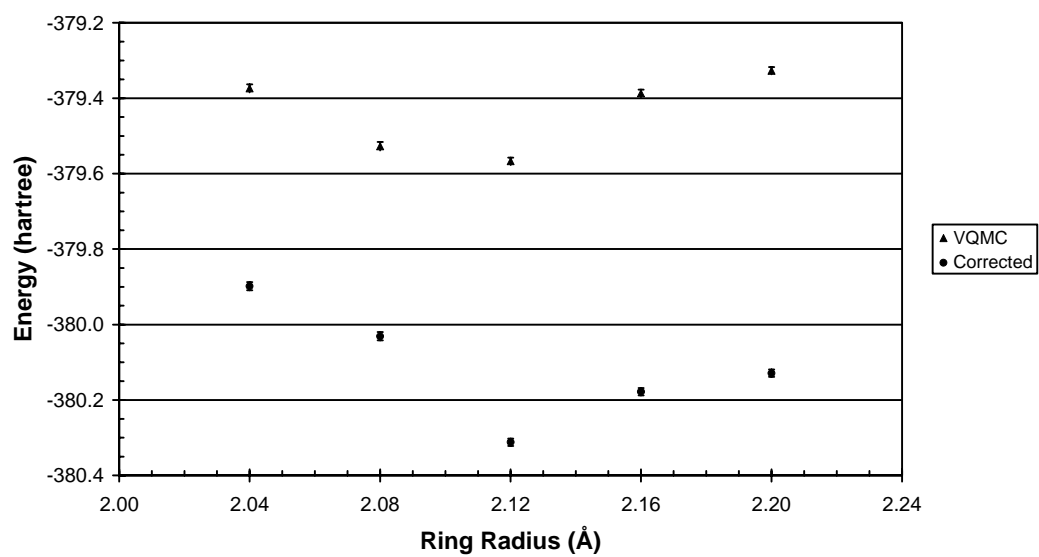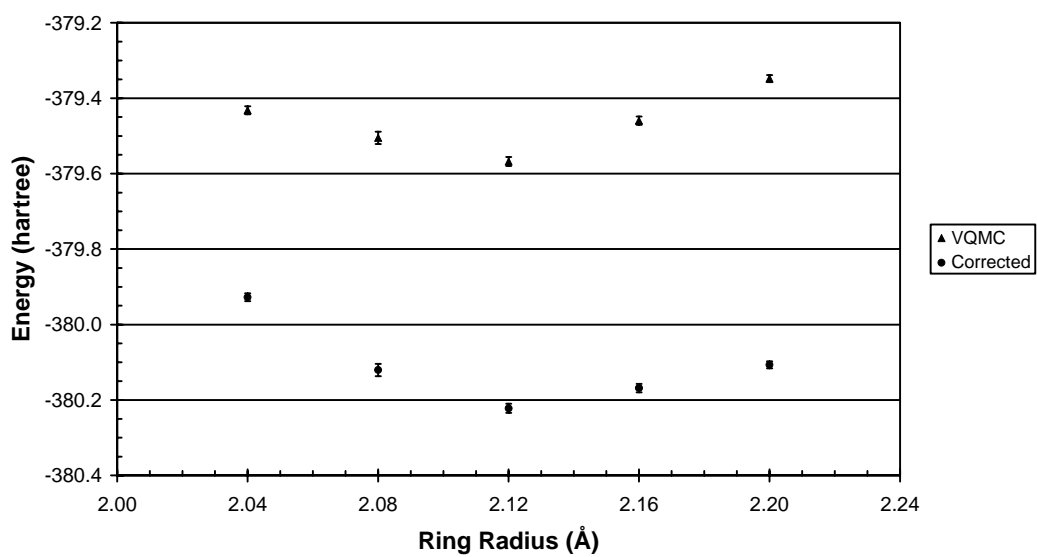

Figure 6.6 VQMC energy and corrected VQMC energy for C_{10} with alternating bond angles of 164° and 124° for various ring radii.
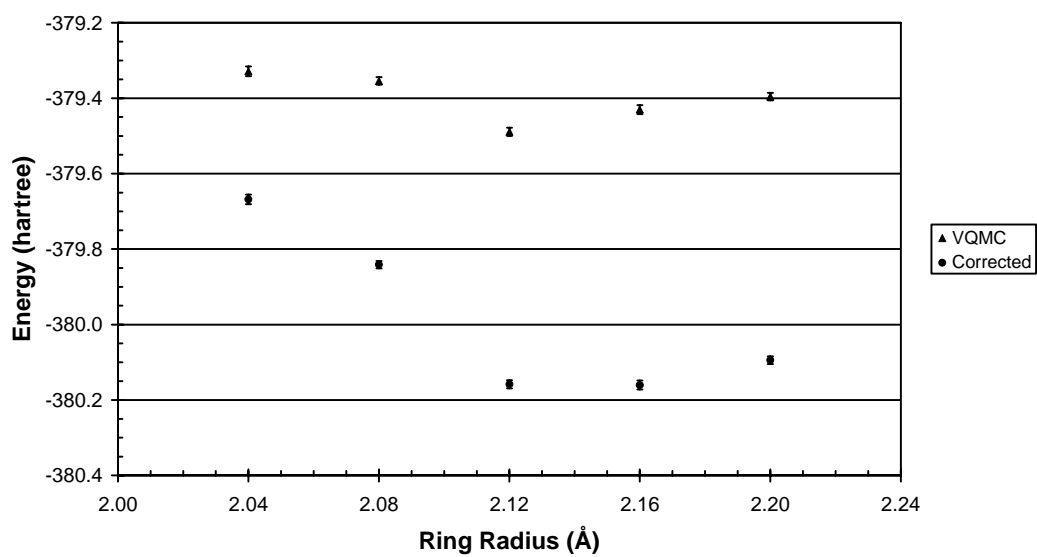
Alternating Bond Angles (112⁰,176⁰)

Figure 6.7 VQMC energy and corrected VQMC energy for C_{10} with alternating bond angles of 176° and 112° for various ring radii.

The results of the VQMC and correction calculations in which all the bond angles are 144° and the bond lengths are alternated for different ring sizes can be found in Tables 6.6 through 6.10.   Figures 6.8 through 6.12 display graphs comparing the VQMC and corrected VQMC energies for C_{10} geometries with increasing bond length ratios for five different ring sizes.

Table 6.6 Correction to the VQMC energy of C_{10} ring with radius 2.04 Å for various bond length ratios.

Bond length ratio	VQMC energy (hartree)	Correction to VQMC energy (hartree)	Corrected VQMC Energy (hartree)
1.000	-379.443(11)	0.9445	-380.387(11)
1.010	-379.457(11)	0.2605	-379.718(11)
1.020	-379.361(11)	0.6621	-380.023(11)
1.030	-379.381(10)	0.8339	-380.215(10)
1.040	-379.462(9)	0.8701	-380.332(9)
1.050	-379.464(10)	0.8796	-380.343(10)
1.060	-379.421(10)	0.6745	-380.096(10)

Table 6.7 Correction to the VQMC energy of C_{10} ring with radius 2.08 Å for various bond length ratios.

Bond length ratio	VQMC energy (hartree)	Correction to VQMC energy (hartree)	Corrected VQMC Energy (hartree)
1.000	-379.534(8)	0.8012	-380.3352(8)
1.015	-379.474(13)	0.7418	-380.2154(13)
1.030	-379.416(8)	0.8329	-380.2493(8)
1.045	-379.457(11)	0.9567	-380.4137(11)
1.060	-379.501(14)	0.7123	-380.2133(14)
1.075	-379.413(12)	0.7054	-380.1184(12)
1.090	-379.359(10)	0.5171	-379.8762(10)

Table 6.8 Correction to the VQMC energy of C_{10} ring with radius 2.12 Å for various bond length ratios.

Bond length ratio	VQMC energy (hartree)	Correction to VQMC energy (hartree)	Corrected VQMC Energy (hartree)
1.000	-379.520(12)	0.7395	-380.2596(12)
1.020	-379.504(11)	0.4303	-379.9340(11)
1.040	-379.462(12)	0.7806	-380.2425(12)
1.060	-379.435(9)	1.1219	-380.5565(9)
1.080	-379.468(12)	0.7434	-380.2118(12)
1.100	-379.432(9)	0.6321	-380.0638(9)
1.120	-379.252(8)	0.7239	-379.9760(8)

Table 6.9 Correction to the VQMC energy of C_{10} ring with radius 2.16 Å for various bond length ratios.

Bond length Ratio	VQMC energy (hartree)	Correction to VQMC energy (hartree)	Corrected VQMC Energy (hartree)
1.000	-379.434(13)	0.5127	-379.9468(13)
1.025	-379.418(11)	0.7292	-380.1469(11)
1.050	-379.438(12)	0.7343	-380.1720(12)
1.075	-379.447(10)	0.6876	-380.1347(10)
1.100	-379.529(14)	0.7202	-380.2495(14)
1.125	-379.440(6)	0.6056	-380.0459(6)
1.150	-379.426(10)	0.4999	-379.9255(10)

Table 6.10 Correction to the VQMC energy of C_{10} ring with radius 2.20 Å for various bond length ratios.

Bond length ratio	VQMC energy (hartree)	Correction to VQMC energy (hartree)	Corrected VQMC Energy (hartree)
1.000	-379.247(10)	0.5577	-379.8051(10)
1.030	-379.408(15)	0.6059	-380.0135(15)
1.060	-379.457(12)	0.8829	-380.3399(12)
1.090	-379.477(6)	0.6634	-380.1402(6)
1.120	-379.462(12)	0.8797	-380.3421(12)
1.150	-379.421(10)	0.7353	-380.1559(10)
1.180	-379.451(9)	0.8460	-380.2968(9)

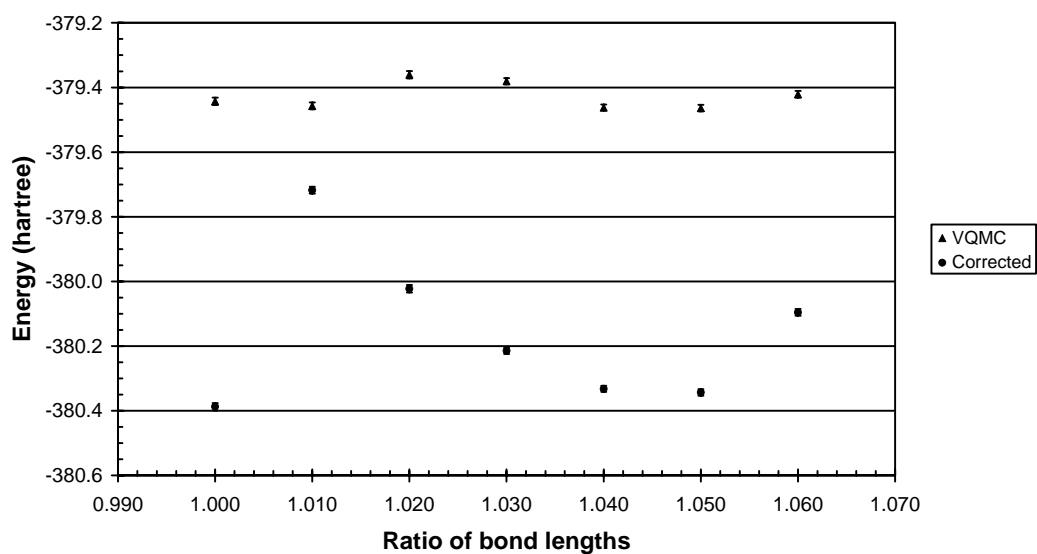**Alternating Bond Lengths (Ring Radius = 2.04 Å)**

Figure 6.8 VQMC energy and corrected VQMC energy for C_{10} with ring radius of 2.04 Å for various bond length ratios.

Alternating Bond Lengths (Ring Radius = 2.08 Å)

Figure 6.9 VQMC energy and corrected VQMC energy for C_{10}
with ring radius of 2.08 Å for various bond length ratios.

Alternating Bond Lengths (Ring Radius = 2.12 Å)

Figure 6.10 VQMC energy and corrected VQMC energy for C_{10} with ring radius of 2.12 Å for various bond length ratios.
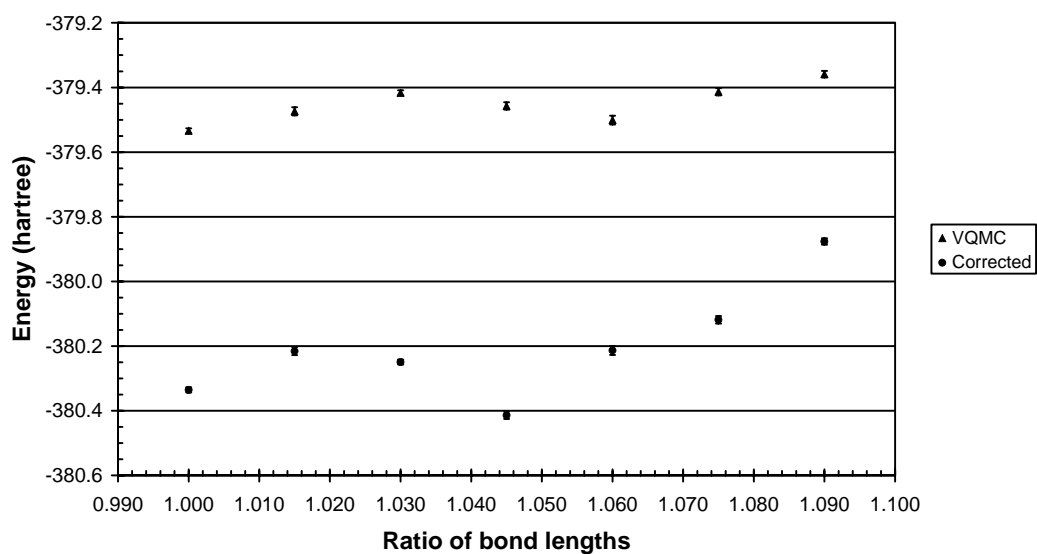
Alternating Bond Lengths (Ring Radius = 2.16 Å)

*Figure 6.11 VQMC energy and corrected VQMC energy for C_{10}
with ring radius of 2.16 Å for various bond length ratios.*
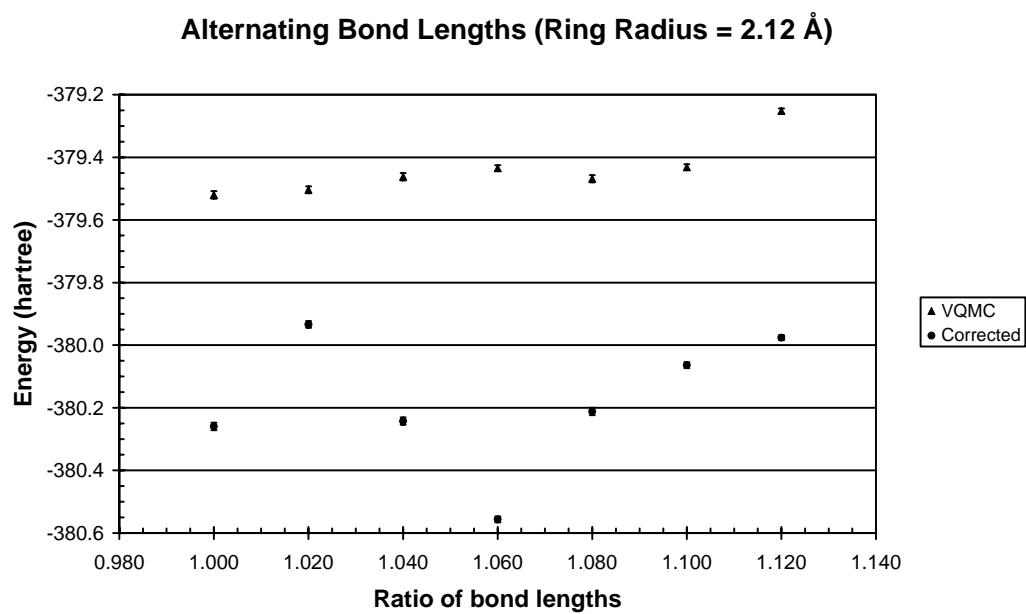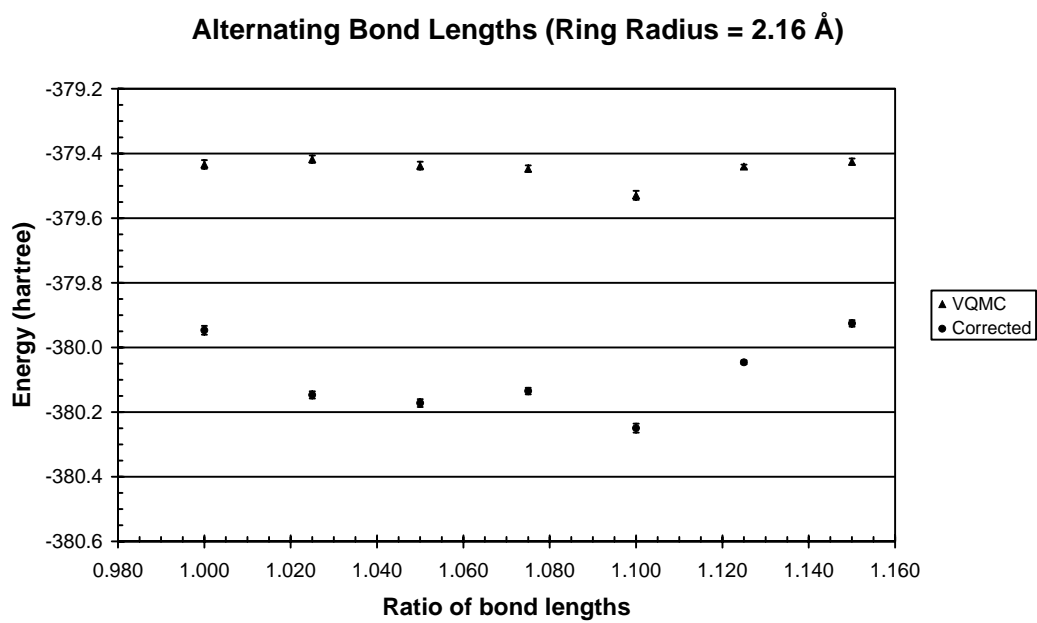
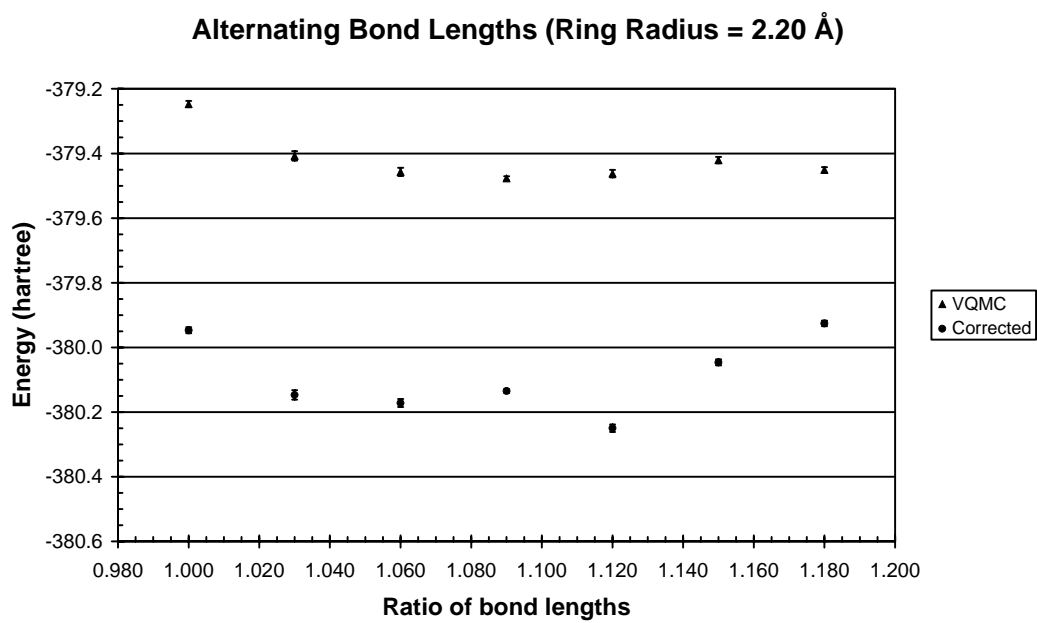**Alternating Bond Lengths (Ring Radius = 2.20 Å)**

Figure 6.12 VQMC energy and corrected VQMC energy for C_{10}
with ring radius of 2.20 Å for various bond length ratios.

Discussion

The correction scheme lowered the VQMC energies by between 0.4 and 1.0 hartree for the ring structure in which the bond angles were varied and all the bond lengths kept equal to each other. For the less distorted rings, with bond angles of (144°,144°) and (148°,140°), the correction to the VQMC energy shows a lower energy for a smaller ring, changing the ring radius with the minimum energy from 2.08 Å to 2.04 Å. For the more distorted rings, the correction to the VQMC energy puts the lowest energy geometry at 2.16 Å for the ring radius, with the exception of (160°,128°), which had the minimum energy at 2.12 Å. This differs from the VQMC results, which had the lowest energy ring radius as 2.12 Å, except for (152°,136°), which had the minimum at 2.16 Å.

For the C_{10} structures in which the bond angles were held at 144° and the bond lengths alternated, the correction scheme lowered the VQMC energies by between 0.25 and 1.15 hartree. The smaller rings showed two minima, one of them at the geometry of a regular decagon. For both the ring radii of 2.04 Å and 2.08 Å, the other minimum fell around a bond length ratio of 1.045. For the structure with a radius of 2.12 Å, the minimum was at a ratio of 1.060. The larger rings did not have a minimum at the regular decagon geometry. The 1.16 Å radius ring had a minimum energy at a bond length ratio of 1.100 and the 1.20 Å ring at 1.120.

An interesting feature of the potential energy curves for the geometry in which the bond lengths are alternated is that for the smaller rings, there is an appearance of two local minima. One minimum is always at the point where the

bond lengths are all equal, forming a regular decagon. This minimum show that there is some stabilization of the molecule due to symmetry and as the symmetry is broken, the energy increases. For the smaller rings, this increase does not continue, but reaches some maximum and then decreases to another minimum. This minimum is also seen for the larger rings, with the minimum at the most symmetric geometry disappearing. This shows that for these larger rings, it is more energetically favorable for the carbons atoms to form pairs, in which two atoms are much closer to each other than in the symmetric geometry and each pair is much farther from the next, than having all the carbon atoms equally spaced in the symmetric geometry. This is the explanation for the second minimum in the potential energy curves for the smaller rings; the rings are small enough that the fully symmetric geometry is stable and is also stable for the carbon atoms to be arranged as pairs in a ring.

REFERENCES

[1] E. Schrödinger, Sitzber. Preuss. Akad. Wiss. Phys.-math. Kl., 144 (1931).

[2] N. Metropolis and S. Ulam, J. Am. Stat. Assoc. **44**, 335 (1949).

[3] M. H. Kalos, Phys. Rev. **128**, 1791 (1962).

[4] H. Conroy, J. Chem. Phys. **41**, 1327, 1331, 1336, 1341 (1964).

[5] N. Metropolis, A. W. Rosenbluth, M. N. Rosenbluth, A. M. Teller, and E. Teller, J. Chem. Phys. **21**, 1087 (1953).

[6] A. Einstein, Ann. Phys. **17**, 549 (1905); **19**, 371 (1906), as reported in Ref. 3.

[7] J. B. Anderson, J. Chem. Phys. **63**, 1499 (1975).

[8] Arnow, D. M., Kalos, M. H., Lee, M. A., Schmidt, K. E. *J. Chem. Phys.* **77**, 5562 (1982).

[9] J. B. Anderson and B. H. Freihaut, J. Comput. Phys. **31**, 425 (1979).

[10] R. C. Grimm and R. G. Storer, J. Comput. Phys. **7**, 134 (1971).

[11] J. B. Anderson, J. Chem. Phys. **73**, 3897 (1980).

[12] Hammond, B. L., Lester, Jr., W. A., Reynolds, P. J., *Monte Carlo Methods in Ab Initio Quantum Chemistry*; World Scientific: Singapore, 1994; pp 133-135.

[13] J. C. Slater, Phys. Rev. **32**, 349 (1928).

[14] J. B. Anderson, J. Chem. Phys. **120**, 9886 (2004).

[15] B. M. Axilrod and E. Teller, J. Chem. Phys. **11**, 299 (1943).

[16] Y. Muto, Nippon Sugaku-Buturigakukai-si **17**, 629 (1943), as reported in Ref. 15

[17] D. Rosen, J. Chem. Phys. **21**, 1007 (1953).

[18] A. Shostak, J. Chem. Phys. **23**, 1808 (1955).

[19] A. E. Sherwood, A. G. De Rocco, and E. A. Mason, J. Chem. Phys. **44**, 2984 (1966).

[20] O. A. Novaro and V. Beltran-Lopez, J. Chem. Phys. **56**, 815 (1972).

[21] C. A. Parish and C. E. Dykstra, J. Chem. Phys. **98**, 437 (1993).

[22] I. Røeggen and J. Almlöf, J. Mol. Struct. **388**, 331 (1996).

[23] V. Mohan and J. B. Anderson, J. Chem. Phys. **92**, 6971 (1990).

[24] G. J. Tawa, P. Whitlock, K. E. Schmidt, and J. E. Moskowitz, Mol. Phys. **77**, 477 (1992).

[25] A. Bhattacharya and J. B. Anderson. J. Chem. Phys. **100**, 8999 (1994).

[26] R. E. Lowther and R. L. Coldwell, Phys. Rev. A **22**, 14 (1980).

[27] M. Bulski and G. Chalasiński, J. Chem. Phys. **86**, 937 (1987).

[28] M. H. Kalos, M. A. Lee, P. A. Whitlock, and G. V. Chester, Phys. Rev. B **24**, 115 (1981).

[29] S. Baroni and S. Moroni, Phys. Rev. Lett. **82**, 4745 (1999).

[30] S. F. Boys and N. C. Handy, Proc. R. Soc. London Ser. A **310**, 63 (1969).

[31] D. C. Clary and N. C. Handy, Phys. Rev. A **14**, 1607 (1976).

[32] K. E. Schmidt and J. W. Moskowitz, J. Chem. Phys. **93**, 4172 (1990).

[33] H. Hartmann and E. Clementi, Phys. Rev. **133**, A1295 (1964).

[34] W. Heitler and F. London, Z. Physik **44**, 455 (1927).

[35] C. A. Couson, Trans. Faraday Soc. **33**, 1479 (1937).

[36] H. Shull and S. Hagstrom, J. Chem. Phys. **30**, 1314 (1959).

[37] B. P. Shoicheff, Can. J. Phys. **35**, 730 (1957).

[38] L. Wolniewicz, J. Chem. Phys. **99**, 1851 (1993).

[39] J. S. Sims and S. A. Hagstrom, J. Chem. Phys. **124**, 094101 (2006).

[40] W. Weltner, Jr. and R. J. Van Zee, Chem. Rev. **89**, 1713 (1989).

[41] J. Bernholc amd J. C. Phillips, Phys. Rev. B **33**, 7395 (1986).

[42] K. Raghavachari and J. S. Binkley, J. Chem. Phys. **87**, 2191 (1987).

[43] C. Liang and H. F. Schaefer, J. Chem. Phys. **93**, 8844 (1990).

[44] J. M. L. Martin and P. R. Taylor, J. Chem. Phys. **102** 8270 (1995).

[45] J. C. Grossman, L. Miras, and K. Raghavachari, Phys. Rev. Lett. **75** 3870 (1995).

[46] Y. Shlyakhter, S. Sokolova, A. Lüchow, and J. B. Anderson, J. Chem. Phys. **110** 10725 (1999).

[47] M. J. Frisch *et al.*, GAUSSIAN 03, (Gaussian Inc., Pittsburgh PA, 2003).

[48] M. W. Schmidt *et al.*, J. Comput. Chem. **14**, 1347 (1993).

VITA

Matthew C. Wilson

Education

2002-2007	Ph.D. in Physical Chemistry
	Pennsylvania State University, State College, PA
1998-2002	B.S. in Chemistry with a minor in Mathematics
	Messiah College, Grantham, PA

Professional Memberships

American Chemical Society
American Physical Society
American Scientific Affiliation
Mathematical Association of America

Papers

Matthew C. Wilson and James B. Anderson, "Quantum Monte Carlo Calculations for Helium Dimers and Trimers", *Advances in Quantum Monte Carlo*, ACS Symposium Series (Pacifichem Conference 2005), in press (2006).

Oral Presentations

2005   "Quantum Monte Carlo Calculations for Helium Dimers, Trimers, and Tetramers"
Pacifichem Conference
Honolulu, HI

Poster Presentations

2006   "Quantum Monte Carlo Calculations for Helium Dimers, Trimers, and Tetramers"
Computation Day
Pennsylvania State University, State College, PA
2005   "Combining Variational and Diffusion Calculations in Quantum Monte Carlo"
ACS National Meeting
Philadelphia, PA